Author Manuscript

Author Manuscript

Author Manuscript

Author Manuscript

HHS Public Access

Author manuscript

Dev Cell. Author manuscript; available in PMC 2023 September 12.

Published in final edited form as:

Dev Cell. 2022 September 12; 57(17): 2048–2062.e4. doi:10.1016/j.devcel.2022.07.016.

Sonic Hedgehog is not a limb morphogen but acts as a trigger to specify all digits in mice

Jianjian Zhu[1], **Rashmi Patel**[1], **Anna Trofka**[1], **Brian D. Harfe**[2], **Susan Mackem**[1,*]

[1]Cancer and Developmental Biology Laboratory, Center for Cancer Research, NCI, Frederick, MD

[2]College of Medicine, Dept of Molecular Genetics and Microbiology and the Genetics Institute, University of Florida, Gainesville, FL

Summary

Limb patterning by Sonic hedgehog (Shh), via either graded spatial or temporal signal integration, is a paradigm for “morphogen” function. Yet how Shh instructs distinct digit identities remains controversial. Here, we bypassed the Shh-requirement in cell survival during outgrowth and demonstrate that a transient, early Shh pulse is both necessary and sufficient for normal mouse limb development. Shh-response is only short-range and limited to the Shh-expressing zone during this time window. Shh patterns digits 1–3, anterior to this zone, by an indirect mechanism, rather than direct spatial or temporal signal integration. Using a genetic relay-signaling assay, we discovered Shh also specifies digit 1/thumb (thought to be exclusively Shh-independent) indirectly, implicating Shh in a unique regulatory hierarchy for digit 1 evolutionary adaptations, such as opposable thumbs. This study illuminates Shh as a trigger for an indirect downstream network that becomes rapidly self-sustaining, with mechanistic relevance for limb development, regeneration, and evolution.

Abstract

[*]lead and corresponding author: mackems@mail.nih.gov.

Author Contributions: SM and JZ designed the project and wrote the paper. JZ, RP, AT, and BDH performed experiments.

Competing interests: None declared.

Publisher's Disclaimer: This is a PDF file of an unedited manuscript that has been accepted for publication. As a service to our customers we are providing this early version of the manuscript. The manuscript will undergo copyediting, typesetting, and review of the resulting proof before it is published in its final form. Please note that during the production process errors may be discovered which could affect the content, and all legal disclaimers that apply to the journal pertain.

Author Manuscript Author Manuscript Author Manuscript Author Manuscript

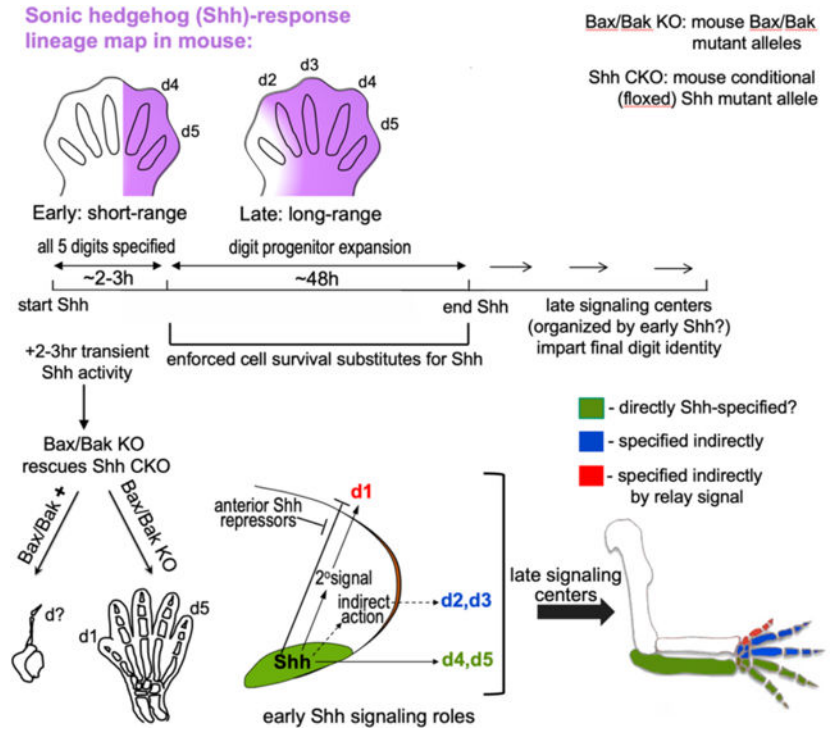

Introduction

Shh is considered a prototypical vertebrate morphogen, with the limb and neural tube serving as a mainstay to elucidate its function. In contrast to neural tube, anterior-posterior (A-P) limb patterning yields different digit identities from a common set of cell types and tissues, with distinct skeletal morphologies that are not based on cell fate changes per se, but arise as an emergent property. Understanding how Shh specifies limb skeletal pattern is central to the problem of structural morphogenesis and informative to regenerative medicine. Shh is secreted by posterior limb bud mesoderm cells defined functionally as the “zone of polarizing activity” (ZPA). Shh/ZPA regulates the specification of distinct A-P digits 2–5 (d2-d5; index to pinky; reviewed by (Zhu and Mackem, 2017), excepting d1 (the thumb), which is thought to form Shh-independently (Chiang et al., 2001). Patterning and growth are coupled; Shh controls both digit type and number during its 2-day limb bud expression span (Figure 1A).

Yet, despite high functional conservation across tetrapods and intense investigation for over two decades, the mechanism by which Shh patterns digits remains controversial. Very disparate models have been proposed in different species with similar limb gene regulatory networks(Harfe et al., 2004; Towers et al., 2008; Yang et al., 1997; Zhu et al., 2008); reviewed by (Zhu and Mackem, 2017). Morphogen-based models of Shh function derive from chick studies showing that changes in concentration or duration can alter both digit identity and numbers, with posterior identities requiring higher concentrations or longer exposures(Scherz et al., 2007; Towers *et al.*, 2008; Yang *et al.*, 1997). Lineage tracing of ZPA-descendants in both chick and mouse have revealed that d4 and d5 arise

Author Manuscript Author Manuscript Author Manuscript Author Manuscript

from the descendants of Shh-expressing ZPA cells(Harfe *et al.*, 2004; Towers et al., 2011), leading to the proposal that temporal integration of short-range Shh, rather than graded long-range signaling, specifies digit identities. Since non-ZPA cells are displaced further away from ZPA signals during outgrowth, the Shh-expressing d4,d5 progenitors receive the longest exposure(Harfe *et al.*, 2004). But the normal coupling of Shh roles in digit identity (patterning) and number (growth) poses a challenge to tease apart the individual requirements for each. Comparing the effects of Shh inhibition with that of cell cycle blockade to reduce digit number in chick(Towers *et al.*, 2008), led to the proposal that temporal signal integration acts to progressively "promote" digit territories to more posterior identity. Yet genetic lineage tracing indicated that Shh-expressing ZPA cells become refractory to Shh-response over time(Ahn and Joyner, 2004), seemingly at odds with temporal integration models to achieve posterior identity. Using a conditional *Shh*-mutant we previously found *Shh* was required for only a limited interval (~8–10 hrs) to specify normal digits; later *Shh* removal caused digit loss in an order that reflected the normal temporal order in which digits arise, and not their AP position(Zhu *et al.*, 2008). Accordingly, the remaining digits that formed were morphologically normal and not transformed to an anterior identity. These results suggested a biphasic model in which Shh is required early for patterning, but over an extended time to promote progenitor survival and expansion, potentially restricting Shh-morphogen action to a more limited time frame.

Here, we use a genetic strategy to uncouple the Shh requirement in digit patterning from expansion/cell survival and test how Shh acts to specify digit pattern. We demonstrate that a transient (~2hr) burst of Shh activity, during which Shh-response is limited to d4-d5 progenitors, suffices to specify all digits normally, implying that non-ZPA derived digits are patterned by an indirect mechanism and that Shh acts neither as a spatial morphogen nor via temporal integration. A genetic assay to test for Shh-induced relay signals unexpectedly reveals that d1 specification is in fact Shh-dependent, requiring an indirect downstream relay signal and highlighting a role for Shh in the evolutionary emergence of a unique, polarized thumb.

Results

A transient Shh pulse restores normal limb development when cell survival is enforced.

To examine the early role of Shh selectively, we used a genetic strategy to uncouple the Shh requirement in digit patterning from that in outgrowth. We asked if enforcing cell survival can bypass late-phase Shh function and restore any digit formation. The pro-apoptotic *Bax*/*Bak* genes(Lindsten et al., 2000) were deleted in *Shh* conditional mutant limb buds exposed to a very transient, early Shh pulse (using $Shh^{C/C}$;Hoxb6CreER, hereafter referred to as *Shh*-CKO, and $Bax^{C/C}$;$Bak^{-/-}$ alleles, referred to as *Bax*-CKO; see Table 1 for list of all crosses and genotypes used). Our analysis focused on hindlimb, where Hoxb6CreER drives complete and robust recombination even prior to limb bud initiation (~E9; see Figure 1A; (Nguyen et al., 2009). Since very early recombination will delete Shh prior to its expression onset, whereas deletion at too late a time will produce only mild digit loss phenotypes even despite reduced cell survival(Zhu *et al.*, 2008), the proper tamoxifen timing to induce Cre and delete *Shh* is critical. Tamoxifen timing was optimized (to E9.5+3hrs;

Author Manuscript Author Manuscript Author Manuscript Author Manuscript

Figure 1B, Table S1) so that 100% of *Shh*-CKO sibling embryos that retained one wild-type *Bax* allele (cell survival not enforced) were invariably *Shh* germ-line null ($Shh^{-/-}$) in hindlimb skeletal phenotype (28/28), providing a clear baseline to assess the effects of bypassing *Shh* late cell-survival function. This tamoxifen timing (at E9.5+3h) rescued digit formation in about 50% of embryos with enforced cell survival (Figure 1D; discussed below) and precedes the normal onset of *Shh* expression by about 9 hours(Lewis et al., 2001; Zhu *et al.*, 2008). Earlier deletion (at E9.5) invariably produced a null phenotype irrespective of enforced cell survival (Table S1), consistent with previous work showing that E9.5 treatment deletes *Shh* efficiently before expression onset(Zhu *et al.*, 2008). At later deletion times (by E9.5+6h), a partial rescue of digit formation occurred even in a portion of embryos without enforced cell survival (*Bax*[+], ~25%, Table S1).

To determine the total duration of Shh signaling activity after optimized tamoxifen treatment (at E9.5+3h), Shh response was assayed by detecting the direct Shh target RNAs (*Gli1*, *Ptch1*)(Litingtung et al., 2002; te Welscher et al., 2002b; Vokes et al., 2008) at one-somite intervals (2 hours per somite (Tam, 1981)) post-tamoxifen treatment (Figures 1C, S1A). Direct target detection is a highly sensitive and earlier read-out for Shh function than is the presence of Shh RNA itself(Lewis *et al.*, 2001; Zhu *et al.*, 2008), and also serves as a sensitive indicator of mosaic recombination at later stages, since residual Shh-expressing cells proliferate over time and would become readily apparent. Analysis of Shh-response at 1-somite intervals after tamoxifen detected a transient 2–3 hour window of Shh activity in about 50% of *Shh*-CKO embryos restricted to the 29 somite stage (7/15 *Ptch1+*, 4/10 *Gli1+*, Figures 1C, S1A). No activity was detected in the remaining 50%, presumably because recombination occurred prior to *Shh* expression onset in those embryos. Notably, transient *Shh* activity is also first detectable in controls at 29 somites (completely absent in all embryos at 28 somites; this study Figures 1C, 3, S1A, S2; in agreement with Zhu et al, 2008; Lex et al 2022). Within two hours later, at the 30 somite stage (+1 somite), when Shh activity (*Ptch1*, *Gli1* expression) is detected in 100% of control ($Shh^{+/-}$) sibling embryos, Shh activity has ceased in all *Shh*-CKO embryos (Figures 1C; S1A) and remains absent subsequently. Analysis of *Shh*-CKO;*Bax*-CKO embryos at multiple later stages also failed to detect the late emergence of any direct target *Gli1* or *Ptch1* expression (see below).

Cell survival was completely restored in 100% of *Shh* mutant limb buds with *Bax*-CKO (20/20, Figure S1B), but notably *Bax*-CKO alone had no effects on limb skeletal patterning in $Shh^{+/C}$;*Bax*-CKO sibling controls (Figure 1D). In *Shh*-CKO;*Bax*-CKO embryos, blocking cell death restored formation of from 3 to 5 digits with normal morphology in about 50% of embryos (18/31, Figure 1D); the remaining 50% retained the $Shh^{-/-}$ null mutant limb phenotype (13/31). The fraction of embryos that did not display any transient Shh activity early (Figures 1C, S1A; Table S1) correlated well with the subsequent frequency having a *Shh* null skeletal phenotype (Figure 1D, Table S1). In *Shh*-CKO;*Bax*-CKO embryos with rescued limbs (18/31), normal long bone morphology (tibia/fibula; zeugopod) was also restored (see also Figure 2C), and normal AP polarity was clearly evident in both the long bones and digits, including distinctive d1 and d5 identities. In contrast, all (100%) of sibling *Shh*-CKO embryos retaining one functional *Bax* allele (*Shh*-CKO;$Bax^{+/C}$) had levels of apoptosis very similar to the $Shh^{-/-}$;$Bax^{+/C}$ (Figure S1B) and later displayed a *Shh* null limb

Author Manuscript Author Manuscript Author Manuscript Author Manuscript

skeletal phenotype with a single dysmorphic digit and malformed zeugopod (28/28, Figure 1D).

These data indicate that a transient early Shh pulse (~2–3h) suffices to specify digit progenitors, but not to maintain cell survival. We next asked if a short Shh pulse is even necessary when cell survival is enforced, using a non-conditional *Shh* null mutant completely devoid of Shh activity (*Shh*$^{-/-}$;*Bax*-CKO). Cell death was completely blocked in *Shh*$^{-/-}$;*Bax*-CKO limbs (9/9, Figure S1B), but enforced cell survival failed to rescue any digit or normal long bone formation (0/18, Figure 1D), even when a non-conditional germ-line *Bax/Bak* mutant (*Shh*$^{-/-}$;*Bax*$^{-/-}$;*Bak*$^{-/-}$) was used to ensure complete *Bax/Bak* inactivation in the *Shh*$^{-/-}$ (0/6 skeletal rescue; Table 1). These results indicate that an early, transient Shh pulse (of 2–3hr) is both necessary and sufficient for normal digit and long bone formation, when the role of *Shh* in maintaining cell survival is bypassed by *Bax/Bak* removal. Consequently, later stage sustained Shh signaling acts mainly to support cell survival and limb bud expansion.

Rescued digits in the early Shh-CKO;Bax-CKO arise from cells that did not respond directly to Shh.

The short 2–3h Shh activity window required for normal limb development when cell survival is enforced is inconsistent with temporal Shh signal integration, but could be compatible with transient activity of a spatially graded morphogen. To assess if Shh acts as a long-range limb morphogen during this early time window in the normal limb bud, we used lineage tracing with *Gli1*$^{CreER/+}$ (Ahn and Joyner, 2004) to track cells that had responded to Shh at early times immediately after *Shh* expression onset. We also compared Shh-response (Gli1CreER activity) with the spatial extent of the Shh-producing ZPA region at the same times (*Shh*$^{CreER/+}$)(Harfe *et al.*, 2004) as a guide in assessing the extent of long-range signaling. Lineage tracing crosses included both *Shh*$^{CreER/+}$ and *Gli1*$^{CreER/+}$ knock-in alleles to genetically mark cells (RosaLacZ reporter activation) in sibling embryos from the same litter that expressed either *Shh*$^{CreER/+}$ or *Gli1*$^{CreER/+}$ alone, ensuring that Shh production and Shh response were compared at identical embryonic ages and tamoxifen exposure times (Figure 2A). A single tamoxifen dose was given at closely spaced early times spanning *Shh* (and *ShhCreER*) expression onset (Figure 2B,C) and limb buds were collected at E13.5, after all digit rays have formed, so that the descendant (LacZ+) cell contributions to different digits can be easily scored (Figure 2A,B).

Genetic LacZ reporter marking revealed that Shh acts only very short-range at early times after expression onset. Notably, the ZPA is highly dynamic; the earliest Shh-expression and response begin in digit 4 territory and then extend to digit 5 progenitors. For tamoxifen treatment times prior to E10.25, Shh response (Gli1CreER activation) was confined to cells that later give rise to d4, d5 (Figure 2B). Long-range signaling was not detected until much later tamoxifen-induction times, initially extending toward d3 (E10.25) and later also including d2 territories (by E10.5, Figure 2B). Yet, tamoxifen treatment at a much earlier stage (E9.5+3h, Figure 1), provides a transient Shh pulse that is both necessary and sufficient to specify all 5 digits if cell survival is enforced. During this time interval, the lineage tracing shows that Shh acts only short-range. Shh response marked by Gli1CreER

Author Manuscript Author Manuscript Author Manuscript Author Manuscript

activity is limited to the Shh-producing ZPA region and directly impacts only d4, d5 progenitors. Consequently, other digit progenitors that do not respond directly to Shh during this time window must be specified by an indirect mechanism (Figure 2C-blue). Notably however, at later stages Shh does act as a long-range signal (by E10.5, Figures 2B and 2C-green), coinciding with the time frame when enforced cell survival (*Bax/Bak* loss) can replace Shh function.

Is the same time frame for short- and long-range Shh signaling also maintained in the *Shh-CKO;Bax-CKO* mutant? The need for a robust, early Cre driver to achieve efficient, rapid deletion in the *Shh-CKO;Bax-CKO* precludes genetic lineage analysis with Cre lines to track Shh response in the mutant context. Gli1LacZ is an alternative response reporter over short time frames (see below), but cannot be used to assess the digit contributions of early responding progenitors. Early-induced LacZ protein does not perdure over the 3-day time interval between transient *Shh* induction and digit ray formation (~E10 to E13.5), and late Gli1LacZ induction by chondrogenesis-associated Ihh in digit rays further confounds interpretation(Witte et al., 2010). To determine if the extent of Shh response relative to early *Shh* expression is similar to wildtype in the *Shh-CKO;Bax-CKO* during the short Shh activity window after tamoxifen treatment (Figure 1), we used hybridization chain reaction (HCR)(Choi et al., 2018) for sensitive, high-resolution spatial detection of *Shh* RNA expression and response (*Gli1* RNA expression) simultaneously, by multiplex labeling in the same limb bud to accurately compare spatial distributions. Note that the *Shh* probes used detect both the recombined (mutant) as well as functional *Shh* transcripts, and that midline hindgut *Ihh* signaling, preserved in the $Shh^{-/-}$ (Zhang et al., 2001), activates some proximal axial response in the urogenital-cloacal region(Haraguchi et al., 2007; Perriton et al., 2002) (see *Shh* and *Gli1* RNAs in Figure 3 $Shh^{-/-}$ panels). Using HCR simultaneous detection, *Gli1*+ response is very similar in its A-P extent to *Shh* and is short range in both sibling controls and *Shh*-CKO*;Bax*-CKO mutants during the transient pulse when response is detected in the mutant limb buds (Figure 3, 29 somite panels, arrows). We also compared spatial A-P extents of *Gli1* and *Ptch1* RNAs by HCR to confirm that the extent coincided for both of the major direct Shh-response reporters (Figure S2). These analyses show that, as in the wildtype, Shh activity/response in the *Shh*-CKO;*Bax*-CKO mutant with rescued digit formation is limited to short-range pathway activation during the transient *Shh* pulse, and restricted to the territory that gives rise only to digit 4–5 (the Shh-expressing ZPA).

Digit Rescue in Shh-CKO;Bax-CKO is not a consequence of residual or re-activated Hh pathway function or pathway target de-repression.

There are several alternative possibilities to account for the observed rescue of normal limb development in *Shh*-CKO;*Bax*-CKO embryos that we excluded. First, a re-emergence of Hedgehog pathway activity, which might be the result of mosaic recombination of the *Shh*-floxed allele, de novo re-induction of a ZPA in a new cell population, or ectopic induction of an alternate Hh ligand. Each of these would result in, and be detected by, re-activation of direct Shh targets (*Ptch1, Gli1* RNA) that provide a more sensitive readout of Hh pathway activity than measuring ligand expression. Monitoring of direct Shh target *Ptch1* (0/7, 0/9) and *Gli1* (0/7) RNAs at both early and late patterning stages, or inclusion of a $Gli1^{LacZ/+}$ knock-in allele (0/8) to provide a highly sensitive Shh-response reporter with

Author Manuscript Author Manuscript Author Manuscript Author Manuscript

enzymatic amplification at early stages(Bai et al., 2002), all failed to detect any Hh pathway recovery in *Shh*-CKO;*Bax*-CKO embryos (Figure 4A). In particular, mosaic recombination of the *Shh*-CKO allele by the transient Cre activity would leave residual Shh-expressing cells that would proliferate and consequently be expected to increase the *Ptch* and *Gli1* reporter signals over time.

Another major, important possibility to address, is potential loss of pathway repression by Gli3 repressor (Gli3R). Shh prevents processing of Gli2/Gli3 nuclear effectors from full-length activators (Gli2FL/Gli3FL; GliA) to truncated repressors (Gli2R/Gli3R) of Shh targets(Wang et al., 2000; Wang et al., 2010). Release from Gli3 repression arguably plays the main role in most Shh limb target regulation(Lewandowski et al., 2015; Litingtung *et al.*, 2002; te Welscher *et al.*, 2002b). Indeed, although *Ptch1* and *Gli1* are direct GliA targets, Gli1 is completely dispensible(Bai *et al.*, 2002) and Ptch1 is not required for digit formation per se once *Shh* expression has begun(Butterfield et al., 2009). Consequently, key limb target activation may occur ligand-independently, without activating Gli1A-target reporters (*Gli1, Ptch1*), via either Gli3R removal or functional antagonism. We used several approaches to test for evidence of altered net Gli3R activity. First, *Hand2*, which induces *Shh*/ZPA by antagonizing *Gli3*(te Welscher et al., 2002a), is directly repressed by Gli3R(Vokes *et al.*, 2008) and remained absent from rescued *Shh*-CKO;*Bax*-CKO in both early (10/10) and later (10/11) stage limb buds (Figure 4A). Secondly, Gli3R activity can be modulated at the protein level by altered processing or degradation(Wang *et al.*, 2000; Wang *et al.*, 2010). Although *Bax/Bak* removal in wildtype limb buds has no impact on skeletal patterning, an altered balance of Bcl2 family members has been reported to affect Gli-processing activity indirectly and could generate a Gli3R deficit(Wu et al., 2017). We examined Gli3 protein levels in early (E10.75) individual limb buds). Gli3FL/Gli3R ratios in *Shh*-CKO;*Bax*-CKO were unchanged from $Shh^{-/-}$;*Bax*-CKO limb buds, and both were equally reduced compared to Shh-expressing controls (Figure 4B), indicating that rescue was not explained by reduced Gli3R protein. Thirdly, “effective” repressor activity of Gli3R may be altered by interacting protein partners without changing quantitative protein level(Chen et al., 2004; Galli et al., 2010). To exclude altered net Gli3R activity by any mechanism, we used a genetic test to compare the phenotypic effect of rescuing cell survival in *Shh*-CKO;*Bax*-CKO with that of intentional *Gli3* dosage reduction. We compared *Bax/Bak* removal with *Gli3* dosage ($Gli3^{+/-}$) effects in both *Shh*-CKO and in $Shh^{-/-}$ limbs. Complete *Gli3* loss alone rescues limb development in $Shh^{-/-}$ embryos, albeit with synpolydactyly and phalangeal morphology changes(Litingtung *et al.*, 2002; te Welscher *et al.*, 2002b). However, haploid *Gli3* dosage ($Shh^{-/-}$;$Gli3^{+/-}$) has an intermediate effect on the $Shh^{-/-}$ null phenotype (improved zeugopod morphology, several small digit rudiments; Figure 4C, 8/8). In contrast to $Shh^{-/-}$;$Gli3^{+/-}$, no change in the $Shh^{-/-}$ null phenotype was observed when *Bax/Bak* was removed (Figure 1D; 18/18). Furthermore, removing *Bax/Bak* in the $Shh^{-/-}$;$Gli3^{+/-}$ limb did not improve limb skeletal phenotype beyond the effect of *Gli3* dosage reduction alone (Figure 4C, 10/10), suggesting that *Bax/Bak* removal did not impact the “effective” net Gli3R level significantly and that reduced *Gli3* dosage, even together with enforced cell survival, in the *Shh* null does not mimic, or substitute for, the effect of transient Shh expression with enforced cell survival (*Shh*-CKO;*Bax*-CKO).

Author Manuscript Author Manuscript Author Manuscript Author Manuscript

Whereas *Bax/Bak* removal had little effect on the $Shh^{-/-}$ null compared to *Gli3* dosage reduction, the reverse holds for the *Shh*-CKO. Without enforced cell survival (*Bax/Bak* removal), the *Shh*-CKO;$Gli3^{+/-}$ was phenotypically identical to the $Shh^{-/-}$;$Gli3^{+/-}$ (12/12; Figure 4C). In contrast, in *Shh*-CKO;*Bax*-CKO limbs with wildtype *Gli3* dosage ($Gli3^{+/+}$), both zeugopod and between 3–5 digits with normal morphologies and clear A-P polarity were restored (18/31; Figures 1D, 4C). Together, these results argue strongly against altered Gli3R activity *per se* as a mechanistic basis for the restoration of normally polarized limb development in the early *Shh*-CKO with enforced cell survival to bypass Shh late function.

Sustained expression of key outgrowth and patterning regulators in Shh-CKO;Bax-CKO with transient Shh activity and enforced cell survival.

To assess whether downstream regulators of limb outgrowth and digit patterning are restored by transient Shh exposure, we examined expression of major direct and indirect downstream Shh targets that regulate limb bud outgrowth (AER/Fgf signaling(Mariani et al., 2008; Zuniga et al., 1999)) and digit patterning (5'*Hox* genes(Davis et al., 1995; Fromental-Ramain et al., 1996)). Unlike *Hand2* and direct GliA-regulated targets (*Ptch1*, *Gli1*), expression of key outgrowth and patterning regulators is maintained in a subset of *Shh*-CKO;*Bax*-CKO embryos, roughly correlating with the observed 50% occurrence of an early, transient Shh activity pulse, and subsequent skeletal rescue (Figures 1, 3, 5, S1, S3). In the remainder, expression profiles in *Shh*-CKO;*Bax*-CKO resembled the null $Shh^{-/-}$;*Bax*-CKO (Figures 5, S3).

The direct Shh target *Grem1* plays a key role in AER/Fgf8 maintenance(Zuniga *et al.*, 1999) and consequently *Fgf8* expression declines in null $Shh^{-/-}$ hindlimb after E10.5(Chiang *et al.*, 2001). $Shh^{-/-}$;*Bax*-CKO limb buds likewise lacked early and late *Grem1* expression (absent in 5/5, 4/4) and by E11.5 *Fgf8* expression was clearly reduced (3/3; Figure 5). In contrast, a subset of *Shh*-CKO;*Bax*-CKO embryos maintained early and late *Grem1* expression (4/10 and 3/7), and preserved *Fgf8* after E10.5 (3/7; Figure 5). The Fgf8-regulated target, *Cyp26b1*, required to clear retinoids for distal limb progression(Probst et al., 2011), was also maintained in *Shh*-CKO;*Bax*-CKO (4/6) but declined in $Shh^{-/-}$;*Bax*-CKO by E11.5 (3/3, Figure S3).

Several 5'*Hox* genes regulate A-P patterning downstream of Shh. *Hoxd13* and *Hoxa13*, critical for digit specification(Fromental-Ramain *et al.*, 1996), are both expressed only at very late stages and at low levels in $Shh^{-/-}$;*Bax*-CKO (3/3, 4/4) compared to controls (Figure 5). In contrast, low level distal *Hoxa13* expression was already detected early in a subset of *Shh*-CKO,*Bax*-CKO hindlimb buds (6/10), and became robust at later stages (5/8). *Hoxd13* was detected at a trace level early (3/8), but was clearly detectable at the onset of the second phase 5'*Hoxd* distal footplate expansion(Tarchini and Duboule, 2006) (4/7, E11.5), and well prior to the late condensation stage after all digit rays have formed, when both the $Shh^{-/-}$ null(Chiang *et al.*, 2001) and $Shh^{-/-}$;*Bax*-CKO re-express *Hoxd13* (~E12.5, Figure S3). Since 5'*Hoxd* genes act mainly during the distal expansion phase to determine digit identity by regulating late interdigit signaling centers(Huang et al., 2016), this sustained second phase *Hoxd13* activation likely suffices for the morphogenesis of normal distinct digit types in *Shh*-CKO;*Bax*-CKO compared to $Shh^{-/-}$;*Bax*-CKO (null) embryos.

Author Manuscript Author Manuscript Author Manuscript Author Manuscript

Hox11 paralogs play a key role in zeugopod patterning and growth(Davis *et al.*, 1995), which is also highly perturbed in the *Shh*$^{-/-}$ but restored in *Shh*-CKO;*Bax*-CKO hindlimbs (tibia/fibula, Figures 1D, 4C). Early *Hoxd11* expression was similar to controls even in *Shh*$^{-/-}$;*Bax*-CKO (2/2), but became undetectable by the second distal expansion phase (2/2). In contrast, *Hoxd11* was maintained at control levels in a subset of *Shh*-CKO;*Bax*-CKO limb buds at both early (5/5) and late (2/7) stages (Figure S3), consistent with zeugopod rescue frequency. Shh inhibition in short term mouse limb bud cultures(Lewandowski *et al.*, 2015; Panman et al., 2006) also suggests that some direct Shh targets are maintained if Shh activity is curtailed after onset, as we have shown here (*Grem1*; *Jag1* in Figures 5, S3). Yet in those studies other downstream targets, particularly 5'*Hoxd* genes, appeared to require sustained Shh activity for their continued expression. However, development does not progress normally in short-term ex vivo cultures, precluding analysis of the second phase 5'*Hoxd* expression (which is selectively restored in the *Shh*-CKO;*Bax*-CKO) in the cultured limb buds after early Shh inhibition.

We also examined the expression of anterior regulators that are repressed/antagonized by Shh activity in posterior limb bud. Unlike the posterior regulators, major anteriorly expressed regulators of patterning, *Irx3*(Li et al., 2014) and *Alx4*(te Welscher *et al.*, 2002b), are only modestly altered in their early extent even in the *Shh* null (*Shh*$^{-/-}$) mutant (Figure S4). However, the slightly extended posterior expression seen in *Shh*$^{-/-}$ was also observed in about 50% of the *Shh*-CKO;*Bax*-CKO embryos (*Irx3* 2/4; *Alx4* 5/8). Our results indicate that expression of targets important for both limb bud outgrowth and patterning are sustained by a transient pulse of Shh with enforced cell survival, providing a basis for the phenotypic rescue of limb development, but do not address the issue of how transient Shh activity leads to stable, graded A-P expression of certain Shh regulated targets in the limb.

Shh is required indirectly to specify digit 1 (thumb).

To test if Shh acts via a relay mechanism, we used a genetic strategy (Figure 6A) to activate Shh targets autonomously only in ZPA cells and ask if any non-ZPA-derived digits are rescued in the complete absence of Shh ligand (*Shh* null). Cell-autonomous pathway activation was achieved using a conditional transgene (*Rosa*^{SmoM2}), expressing a constitutively-active form of Smoothened (SmoM2)(Jeong et al., 2004), a membrane GPCR essential for transducing Shh(Kong et al., 2019). The *Shh*^{Cre} knock-in allele(Harfe *et al.*, 2004) was used to restrict SmoM2 and Shh-target activation to ZPA cells (*Shh*^{cre};*Rosa*$^{SmoM2/+}$; referred to as Shh-SmoM2+), and evaluated in the *Shh* null background (*Shh*$^{cre/-}$). Enforced Shh-response by SmoM2 in the ZPA also affects Ihh targets and chondrogenesis(Long et al., 2001), precluding morphologic evaluation of any ZPA-descendant digits (d4,d5 in wildtype), but differentiation of non-ZPA digits is unaffected (d1-d3, see Figure S5A). Unexpectedly, in both *Shh*$^{cre/-}$ fore- and hindlimbs, enforced, cell-autonomous pathway activation of *Shh*$^{cre/-}$;Shh-SmoM2 in the ZPA rescued formation of a positionally and morphologically normal, biphalangeal digit 1 at high frequency (66%; 21/32 limbs, Figure 6B). Digit 1 specification is thought to be Hh-independent, based on the normal lack of any direct Shh-response in the d1 progenitor territory(Ahn and Joyner, 2004) (see also Figure 2B) and the persistence of a d1-like structure in *Shh* null hindlimbs(Chiang *et al.*, 2001). However, our genetic lineage tracing reveals that the single dysmorphic digit

Author Manuscript Author Manuscript Author Manuscript Author Manuscript

in the *Shh* null mutant (*Shh*$^{cre/-}$) is actually entirely descended from posterior ZPA (LacZ+) d4/d5 progenitor cells (Figures 6C, S5A), which lies outside of and posterior to the zone of broad anterior apoptosis present in *Shh*$^{-/-}$ limb buds (Figures S1B, S5D,E; see also (Chiang *et al.*, 2001; Zhu *et al.*, 2008)). In contrast to the posterior ZPA-origin of the single *Shh*$^{-/-}$ null hindlimb digit, our lineage analysis clearly demonstrates that the morphological "d1" rescued in the *Shh*$^{cre/-}$;Shh-SmoM2 arises non-autonomously entirely from anterior (LacZ-negative) non-ZPA limb cells (5/5; Figure 6C) and condenses at the anterior limb margin where d1 normally forms (see Figure S5F). Digit 1 rescue was not the result of either cryptic Hh ligand or downstream pathway activation as seen in a small fraction of control Shh-SmoM2+ limb buds (*Gli1*, 0/8; *Ptch1*, 0/10; Figure S5A,C). Distal-anterior *Hoxa13* expression, which is uniquely essential for d1 specification(Bastida et al., 2020; Fromental-Ramain *et al.*, 1996), and is absent or greatly reduced in *Shh*$^{Cre/-}$ null (0/4), was restored across the *Shh*$^{cre/-}$;Shh-SmoM2+ distal limb bud (6/6; Fig. 6D), confirming d1 identity. Likewise, a late d1-specific marker (*Uncx4.1*) was also expressed in the rescued digit domain of *Shh*$^{cre/-}$;Shh-SmoM2 (6/8), but not in *Shh*$^{Cre/-}$ (0/4; Figure S5B). Together, these results strongly argue that a bona fide digit 1 is absent in the *Shh* null mutant but is restored in the *Shh*$^{cre/-}$;Shh-SmoM2, indicating that d1 specification is indirectly Shh-dependent and requires a relay signal that is activated downstream of Shh-response in the ZPA.

Why was only d1, but not other non-ZPA digits (d2,3) restored by Shh-SmoM2? Shh cell-survival function remains absent and *Shh*$^{cre/-}$;Shh-SmoM2+ limb buds display considerable anterior apoptosis (Figure S5D,E), but enforcing cell survival (with *Bax*$^{-/-}$;*Bak*$^{-/-}$, see Table 1) did not rescue any further digit formation besides d1 (8/8). We suspect that the failure to rescue d2–3 reflects a problem inherent in the timing of enforced SmoM2/Shh-response in ZPA cells (which is induced by *Shh*^{Cre} only after normal *Shh* onset). The delayed specification timing of d1 relative to other digits(Bastida *et al.*, 2020) would be consistent with this selective d1 rescue.

Discussion

Our genetic rescue reveals two distinct roles for Shh in the limb: a transient (2–3hr), early requirement that is critical to specify all digits, and a sustained requirement to promote cell survival. This transient Shh pulse is both necessary and sufficient for normal limb morphogenesis, if the role of Shh in maintaining cell survival is bypassed (by *Bax/Bak* removal). Yet genetic lineage tracing, together with HCR, shows that Shh-response is short-range and restricted to ZPA-derived digit progenitors (d4-d5) during the same time window of transient Shh activity that suffices to specify all digits. Both biochemical and genetic assays reveal that the Gli3R activity gradient is unperturbed by the short Shh activity window in the rescued *Shh*-CKO;*Bax*-CKO, consistent with the absence of any long-range Hh response. Together, these results indicate that Shh is not a limb morphogen but acts via an indirect mechanism to specify the non-ZPA digits (d1–3, Figure 6E). Shh may act locally to specify d4/5 directly, but our results don't exclude an indirect contribution. Digit 1 specification, occurring relatively late, is further distinguished in being repressed by direct Shh response, yet indirectly Shh-dependent via a relay signal (discussed below). These different responses to Shh signaling define up to three distinct types of regulation leading

Author Manuscript Author Manuscript Author Manuscript Author Manuscript

to: specification of posterior ZPA-descended digits (4,5), anterior digits (2–3), and digit 1 (Figure 6E). Unexpectedly, long-range Shh signaling, which occurs only at later stages when the limb bud is expanding and well after specification is complete, plays a critical role in sustaining cell survival across the d2–5 territories. We previously showed the number of digits lost decreases progressively with later Shh deletion times, correlating with later onset of apoptosis ((Zhu *et al.*, 2008); see also Table S1), but the entire late Shh requirement is completely bypassed by Bak/Bax removal in the early *Shh*-CKO.

We considered the possibility that either persistent low-level, residual pathway activity, or a long-range response during the transient *Shh* expression pulse had escaped detection, but think this unlikely for the following reasons. 1) Low-level Shh activity persistence, owing to either incomplete *Shh* recombination or some compensatory feedback leading to ectopic Hh ligand activation should all result in the continued activation of direct targets *Gli1* and *Ptch1*, which are detectable at much lower levels than is *Shh* RNA(Lewis *et al.*, 2001; Lex et al., 2022; Zhu *et al.*, 2008). Furthermore, Shh-expressing cells proliferate in the early limb bud to give rise to d4/d5, and activation of direct target reporters should be increasingly apparent over time (E10.5-11.5). Several methods (including reporter amplification steps; HCR, Gli1LacZ) failed to detect any Shh response in *Shh*-CKO;*Bax*-CKO limbs (Figures 1C, 3, 4A, S1), either by 3 hrs after *Shh* expression onset (28/28), at 12 hrs after onset (26/26), or at 36 hrs (16/16) nearing the end of normal *Shh* duration. 2) The skeletal phenotype of *Bax*+ *Shh*-CKO sibling embryos was uniformly identical to the *Shh* germline null (28/28, Figure 1D), which is incompatible with residual Shh signaling. Persistent, low level Shh (generated by deleting *Shh* with *ShhCre*) results in a very mild digit phenotype (16/16) and modest *Ptch1* response(Scherz *et al.*, 2007), despite only trace levels of *Shh*. 3) Long-range signaling effects on Gli3R activity (target de-repression) were not detected. Many Shh targets are regulated mainly by de-repression(Lewandowski *et al.*, 2015; Lex et al., 2020), but long-range effects of Shh on Gli3R and target “de-repression” are not measured by GliA-dependent target reporters (*Gli1, Ptch1*). There is no single, uniform expression response for this target class, and consequently no good universal “reporters” to assay Shh-induced de-repression, because regulation of derepressed targets by other activating transcription factors varies highly from gene to gene(Lewandowski *et al.*, 2015). But phenotypic comparison to the effects of Gli3 dosage reduction can serve as a gauge to assess perturbation of the anteriorly-biased Gli3R gradient caused by long-range signaling and target de-repression during transient Shh activity. We altered genetic Gli3 dosage to assess if *Shh*-CKO;*Bax*-CKO rescue might result from altered Gli3R activity. Our results (Figure 4C) indicate that *Gli3* dosage reduction ($Gli3^{+/-}$) does not phenocopy the digit rescue by enforced cell survival in the *Shh*-CKO, and has no impact on the *Shh*-CKO skeletal phenotype beyond the effect of $Gli3^{+/-}$ on the $Shh^{-/-}$ null mutant, arguing against long-range modulation of Gli3R by transient Shh signaling in the rescued *Shh*-CKO. Similarly, long range GliA response detection relies on two targets, *Ptch1* and *Gli1* (reported by HCR and by Gli1CreER). Given the limited repertoire of Hh-response reporters, we cannot definitively exclude a transient morphogen action of Shh at levels below their detection thresholds.

Digit identity is morphologic in nature, arising via distinct organizations of the same tissues and not based in cell fate changes, features suggesting progressive specification. Indeed,

Author Manuscript Author Manuscript Author Manuscript Author Manuscript

work in both chick and mouse indicates that late interdigit signaling centers impinge on digit tip progenitors to regulate phalanx numbers formed, determining final digit identities(Dahn and Fallon, 2000; Huang and Mackem, 2021; Huang *et al.*, 2016; Suzuki et al., 2008; Witte *et al.*, 2010). Shh may regulate digits specified at particular A-P limb positions via relay signals to establish such late signaling centers (Figure 6E). If Shh acts early as a trigger, it is not surprising that direct targets involved in signal transduction and response range modulation, such as Gli1 and Ptch1, become dispensable when cell survival is enforced. In contrast, downstream targets that regulate growth, such as Grem1, and later patterning, such as Hoxa13 and Hoxd13, appear to play key roles; their maintenance correlates with the limb rescue frequency by a transient Shh pulse.

Uncovering the mechanisms that sustain stable gene activation after only transient Shh exposure will be an important future focus to illuminate how Shh patterns the developing limb. Stable alterations in target gene expression following transient Shh exposure could involve several, non-mutually exclusive mechanisms including chromatin and/or DNA modifications and relay mechanisms incorporating lock-on circuitry(Alon, 2007). Recent work suggests that Shh targets are poised for expression as soon as Shh activity initiates and that Gli3-mediated repression commences only after this point(Lex *et al.*, 2020; Lex *et al.*, 2022). A transient burst of Shh activity could trigger a self-reinforcing bi-stable switch(Alon, 2007) if activating factors that reinforce target expression also block introduction of repressive marks by Gli3R post-Shh onset. One type of indirect mechanism would be via non-cell autonomous relay signals acting downstream of transient Shh activity to specify non-ZPA derived digits. Such relay signals can become rapidly self-sustaining via feedback loops, as occurs with Fgf10-Fgf8 signaling downstream of transient Tbx5 activity in the limb(Hasson et al., 2007). Other indirect mechanisms that remain less extensively explored, such as bioelectric or mechanical, are also possible(Harris, 2021; Piccolo et al., 2022).

One alternative to a relay mechanism for patterning digit territories not directly responsive to transient Shh signaling would be the maintenance of polarity, once initiated by transient Shh activity, at the level of antagonistic interactions between “posterior” (Shh target) and “anterior” (antagonizing) transcription factors, which are initially co-expressed in very early-stage limb bud mesenchymal cells(Osterwalder et al., 2014). However, such a scenario is difficult to reconcile with the finding that A-P polarized expression of some, but not other, targets is maintained in the rescued *Shh*-CKO;*Bax*-CKO limb buds and is accomplished in the absence of any *Hand2* expression, which normally antagonizes anterior Gli3R to maintain posterior limb bud asymmetry downstream of Shh(te Welscher *et al.*, 2002a). Furthermore, lineage tracing indicates that the response to “transient” Shh is entirely restricted to the posterior ZPA, which would generate clear-cut anterior and posterior limb bud compartments, rather than the graded A-P target gene expression seen for some target genes maintained in the rescued *Shh*-CKO;*Bax*-CKO (eg. *Grem1, Hoxa13*, Figure 5). Spatially graded target expression would require some type of non-autonomous effect, whether induced by Shh effectors (Gli2/3), or by other transcription factors acting downstream of short-range Shh response within the ZPA.

Author Manuscript Author Manuscript Author Manuscript Author Manuscript

Whether Shh acts as a trigger, via an indirect mechanism, to specify digits has implications for both limb evolution and regeneration. Such an indirect mechanism is at odds with chick studies showing that Shh acts as a limb morphogen(Scherz *et al.*, 2007; Towers *et al.*, 2008; Yang *et al.*, 1997). These studies rely on pharmacologic inhibition that may persist to later stages to affect Ihh in digit tip progenitors, leading to phalanx loss(Gao et al., 2009) that scores as digit identity changes attributed to Shh inhibition; reduced cell survival by Shh suppression may also impact late-stage digit morphogenesis. Other chick studies suggested involvement of downstream relay signals(Drossopoulou et al., 2000; Pickering et al., 2019; Yang *et al.*, 1997) , but did not discriminate if Shh also acts as a morphogen. Whether apparent mouse-chick differences in Shh function reflect biologic or technical factors remains to be explored and will be important for understanding the degree of functional conservation in assessing evolutionary adaptation (for eg. proposed Shh role in thumb evolution, below). Our results indicating Shh acts mainly to promote cell survival after a transient requirement in specification also support the proposal that regulation of digit number and pattern by Shh can be uncoupled to facilitate adaptive evolution of digit number(Shapiro et al., 2003; Zhu *et al.*, 2008). Shh acting as a short-range trigger in developing limb may also be more parsimonious with patterning events during limb regeneration(Nacu et al., 2016). Although Shh is implicated in AP patterning during axolotl limb regeneration, inductive interactions overall appear to be mainly short-range with little evidence for long-range morphogen function.

Our genetic relay signal assay, selectively enforcing Shh response solely in the ZPA of the Shh null ($Shh^{-/-}$) mutant, unexpectedly revealed that d1 is indirectly Shh-dependent. The rescued digit arose entirely from non-ZPA anterior cells, and had all the features of bona fide digit 1 based on positional, morphologic, and gene expression criteria. Yet previous work has shown that direct Shh response selectively prevents formation of d1 territory, and indeed, a complex regulatory circuit that represses *Shh* anteriorly is required to specify d1(Li *et al.*, 2014). Unlike other digits, the d1 territory also remains outside of the Shh signaling-response range (eg. Figure 2B) during the entire expansion phase when Shh maintains cell survival. Consequently d1 survival is sustained differently. Why impose such a complex regulatory hierarchy for d1 formation (see Figure 6E), involving repression by direct Shh signaling but requiring an indirect Shh-induced relay signal? We propose that the unique control and consequent delay in d1 specification and growth/expansion enabled its independent evolution by uncoupling its regulation and morphogenesis from that governing other digits. Such regulatory uncoupling would facilitate the evolution of an opposable thumb, as well as other grasping/clutching adaptations important for arboreal tetrapods, including birds and mammals.

Limitations of the Study.

Shh-response reporters showing that Shh acts only at short range and not beyond the ZPA in early limb bud may have failed to detect a very low level, transient longer-range activity. Restricted, short-range, early stage Shh activity and skeletal phenotypic outcome cannot be evaluated in the same embryo in *Shh*-CKO rescue experiments; the relationship remains correlative, albeit strongly so. Definitive demonstration that Shh acts indirectly, as a trigger rather than a morphogen, to pattern limb digits will require identifying the factors involved.

Author Manuscript Author Manuscript Author Manuscript Author Manuscript

STAR METHODS

RESOURCE AVAILABILITY

Lead contact—Further information and requests for resources and reagents should be directed to and will be fulfilled by the lead contact, Susan Mackem (mackems@mail.nih.gov)

Materials availability—The *Bax*-deleted ($Bax^{+/-}$) mouse line generated in this study can be obtained from the lead contact, Susan Mackem.

Data and Code Availability

Data: All microscopic and other imaging data reported in this paper will be shared by the lead contact upon request.

Code: No bioinformatic data or code were generated.

Any additional information required to reanalyze the data reported in this paper is available from the lead contact upon request.

EXPERIMENTAL MODEL AND SUBJECT DETAILS

Mice—All animal studies were carried out according to the ethical guidelines of the Institutional Animal Care and Use Committee (IACUC) at NCI-Frederick under protocol #ASP-20-405. All mice were maintained in a specific pathogen-free facility with a 12-hr light cycle (6 am-6 pm) on a standard chow diet (LabDiet mouse breeder diet O/HS). Both male and female mice with mutant alleles displayed no sex differences in phenotypes, and embryos of both genders ranging from E9.5-17.5 were included in all analyses, but individual gender determination was not carried out. The *Shh*-floxed(Lewis *et al.*, 2001), *Shh* null(Chiang et al., 1996), *Bax*-flox;$Bak^{-/-}$(Takeuchi et al., 2005), $Gli1^{LacZ/+}$(Bai *et al.*, 2002), and *Gli3* (*Xt-J*)(Buscher et al., 1998) mutant lines, and the *Hoxb6*CreER(Nguyen *et al.*, 2009), *Shh*Cre(Harfe *et al.*, 2004), *Shh*CreER(Harfe *et al.*, 2004), *Gli1*CreER(Ahn and Joyner, 2004), *Rosa*SmoM2(Jeong *et al.*, 2004), *Rosa*LacZ(Soriano, 1999), and *Rosa*EYFP(Srinivas et al., 2001) mouse lines were all described previously. All single and compound mouse lines were maintained on an outbred, mixed strain background (predominantly FVB/n and C57BL/6). A detailed summary of the crosses used to generate embryos for different experiments and outcomes is provided in Table 1. For timed matings, noon on the date of the vaginal plug was defined as E0.5. For phenotypic rescue with *Hoxb6*CreER, pregnant mice were injected intraperitoneally with a single dose of 3mg tamoxifen and 1mg progesterone (Nakamura et al., 2006) at E9.5+3hrs and embryos were collected at times indicated. Somite numbers were counted at time of collection for embryos that were harvested before E10.5. Sibling embryos were used in comparative analyses whenever possible. For lineage tracing with *Shh*CreER and *Gli1*CreER, a single dose of 0.5–1mg tamoxifen was injected at the times indicated.

Bax-deleted ($Bax^{+/-}$) mice were generated by crossing *Bax*-flox males with *Prrx1*Cre(Logan et al., 2002) females to produce germ-line recombination and offspring were out-crossed to

Author Manuscript Author Manuscript Author Manuscript Author Manuscript

remove *Prrx1*Cre and then crossed with the lines listed in Table 1. The *Bax*-deleted allele genotype was detected using PCR (see Key Resources Table for primers).

METHOD DETAILS

Determination of embryo ages for Shh-response onset and loss in *Shh*-CKOs —To determine embryo ages for Shh-response onset and loss in *Shh*-CKOs (Figures 1, 3, S1), somite numbers were counted at the times of embryo collection. At this stage, somites form at a predictable rate of 1 somite every 2 hours(Tam, 1981) and our results in Figures 1, 3, S1, S2. Somite numbers present at time of tamoxifen injection were calculated retrospectively (Figure 1B), based on the actual somite number present when the embryos were collected several hours later for analysis. Somite number of embryos at a given collection time showed some variation (+/− 1 somite) and this was reflected in the time range of CreER-mediated recombination shown in Figure 1B. Somite-matched controls and *Shh*-CKOs came from the same litters to ensure the same tamoxifen treatment conditions. Importantly, the first appearance of *Shh* activity/response (*Ptch1* and *Gli1* RNA) in hindlimb buds reproducibly occurred at 29 somites, consistent with both our previous detailed time-course analysis and with other reports(Lewis *et al.*, 2001; Lex *et al.*, 2022; Zhu *et al.*, 2008). Shh inactivation in *Shh*-CKOs, determined by the absence of *Ptch1* and *Gli1* expression compared to control siblings, was consistently 100% by 30 somites (within 2 hrs of first detection).

Whole mount *in situ* hybridization—Hybridizations were carried out following a previously described detailed protocol(Wilkinson, 1992). Embryos were fixed in 4% w/v paraformaldehyde in PBS overnight at 4°C, washed in PBS, gradually changed to absolute methanol and bleached in 5:1 methanol/30% hydrogen peroxide for 2 hrs at room temperature, and stored in methanol at −20°C until hybridization. Embryos with different genotypes were treated together, in one tube, with 20ug/ml proteinase K in PBS for 8–16 mins based on the embryo age (this step was omitted for *Fgf8* probe). Gene-specific, digoxigenin-UTP labeled probes were synthesized from cDNA templates and incubated with embryos in hybridization buffer with 50% v/v formamide overnight at 70°C. The embryos were then washed with a series of buffers and incubated in alkaline-phosphatase-conjugated antidigoxigenin antibody overnight at 4°C. After washing with 0.1% v/v Tween in Tris buffered saline, embryos were incubated in BM purple or in 350 ug/ml NBT and 175 ug/ml BCIP in Tris buffered saline (pH 9.5) to detect hybridized RNA.

Hybridization chain reaction (HCR) *in situ* analysis—Mouse embryos were fixed, bleached, and stored the same way as described in the whole mount *in situ* hybridization above. Whole mount *in situ* hybridization of limb buds at ages indicated was performed using recommended conditions and solutions for third generation hybridization chain reaction (HCR) probes(Choi *et al.*, 2018) designed by Molecular Instruments (Los Angeles, CA) and analyzed by confocal microscopy. Maximum projection images of fluorescence intensity from confocal image stacks spanning the entire dorsoventral limb bud thickness were generated to compare the A-P extent of Shh, Gli1 and Ptch1 RNA signals. For both Figures 3 and S2, all image panels are shown at the same scale, with scale bar of 100μm.

Author Manuscript Author Manuscript Author Manuscript Author Manuscript

Skeletal staining—For skeletal staining(Kessel and Gruss, 1991), embryos were collected at E15.5-E17.5, eviscerated and fixed in absolute ethanol overnight, followed by absolute acetone overnight, and by staining in 150 ug/ml alcian blue and 50 ug/ml alizarin red in 95% v/v ethanol in H_2O overnight. After clearing in 1% w/v KOH in H_2O for several hours followed by 1% KOH w/v in 20% v/v glycerol in H_2O, embryos were stored and imaged in 50% v/v glycerol in H_2O.

Lysotracker staining—Embryos were collected in PBS and immediately incubated in 5uM lysotracker red in PBS with calcium and magnesium for 30 mins at 37°C. Embryos were then washed in PBS and fixed in 4% w/v paraformaldehyde in PBS overnight at 4°C. Embryos were washed in PBS, transferred to absolute methanol in graded steps and cleared in 1:2 v/v benzyl alcohol/benzyl benzoate (BABB) solution to visualize staining.

Western blot and quantification analysis—For western blot analysis, one pair of hindlimb buds from individual E10.75 embryos were dissected in PBS, lysed and sonicated in 1x NuPAGE LDS sample buffer with 1% w/v SDS and proteinase inhibitors. Reducing agent was added and samples were heated to 95 °C for 10 mins before loading. Two hindlimb buds (from 1 embryo) were loaded per lane, and electrophoresed in NuPAGE 3–8% Tris-Acetate protein gels. Proteins transferred to nitrocellulose membranes were probed with either affinity-purified polyclonal rabbit anti-Gli3(Chen *et al.*, 2004) or goat polyclonal anti-Gli3 (1:1000, R&D, AF3690) and mouse anti-vinculin (1:1000, Sigma, V9264) and visualized with fluorescent secondary antibodies (1:10,000, LI-COR IRDye 800CW, 926-32211, anti-rabbit green; 926-32214, anti-goat green; and with #680RD, #926-68072, anti-mouse red) using LI-COR Odyssey CLx. Band intensities were quantified with Image Studio software v5.2. Number of independent samples analyzed for each genotype is listed in Fig. 4. For statistical analysis of western data (Gli3 FL/R), standard 2-sided t-test was used to calculate p values. Levels of alpha in t-tests <0.05 are considered significant.

Beta-galactosidase (LacZ) staining—Embryos were fixed in 2% w/v paraformaldehyde with 0.2% v/v glutaraldehyde for 1h at 4°C, washed in PBS with 0.1% v/v Tween (PBT) and stained with XGal (1mg/ml) in PBT and 2mM $MgCl_2$, 5mM Ferro-CN, 5mM Ferri-CN, at 37 °C for several hours.

QUANTIFICATION AND STATISTICAL ANALYSIS

For immunoblots, Image Studio software v5.2 in the LI-COR Odyssey CLx system was used to quantify band fluorescence signals. Statistical significance of differences was determined using the standard 2-sided t-test. Numbers of biological replicates, means, SEM, and p values for immunoblots are reported in the main text and/or figure legends. Levels of alpha in t-tests <0.05 are considered significant.

Supplementary Material

Refer to Web version on PubMed Central for supplementary material.

Author Manuscript Author Manuscript Author Manuscript Author Manuscript

Acknowledgements:

We thank Cliff Tabin and Marian Ros for stimulating discussions and critical reading of the manuscript and Sohyun Ahn, Chin Chiang, Alex Joyner, Andy McMahon, Cliff Tabin, Heiner Westphal and Yingzi Yang for providing mouse lines.

Funding:

This research was supported by the CCR, NCI (to SM, Intramural Research Program).

Data and materials availability:

All data is available in manuscript and supplementary materials.

References

Ahn S, and Joyner AL. (2004). Dynamic changes in the response of cells to positive hedgehog signaling during mouse limb patterning. Cell 118, 505–516. 10.1016/j.cell.2004.07.023. [PubMed: 15315762]

Alon U. (2007). An introduction to systems biology : design principles of biological circuits (Chapman & Hall/CRC).

Bai CB, Auerbach W, Lee JS, Stephen D, and Joyner AL. (2002). Gli2, but not Gli1, is required for initial Shh signaling and ectopic activation of the Shh pathway. Development 129, 4753–4761. [PubMed: 12361967]

Bastida MF, Perez-Gomez R, Trofka A, Zhu J, Rada-Iglesias A, Sheth R, Stadler HS, Mackem S, and Ros MA. (2020). The formation of the thumb requires direct modulation of Gli3 transcription by Hoxa13. Proc Natl Acad Sci U S A 117, 1090–1096. 10.1073/pnas.1919470117. [PubMed: 31896583]

Buscher D, Grotewold L, and Ruther U. (1998). The XtJ allele generates a Gli3 fusion transcript. Mamm Genome 9, 676–678. 10.1007/s003359900845. [PubMed: 9680393]

Butterfield NC, Metzis V, McGlinn E, Bruce SJ, Wainwright BJ, and Wicking C. (2009). Patched 1 is a crucial determinant of asymmetry and digit number in the vertebrate limb. Development 136, 3515–3524. 10.1242/dev.037507. [PubMed: 19783740]

Chen Y, Knezevic V, Ervin V, Hutson R, Ward Y, and Mackem S. (2004). Direct interaction with Hoxd proteins reverses Gli3-repressor function to promote digit formation downstream of Shh. Development 131, 2339–2347. 10.1242/dev.01115. [PubMed: 15102708]

Chiang C, Litingtung Y, Harris MP, Simandl BK, Li Y, Beachy PA, and Fallon JF. (2001). Manifestation of the limb prepattern: limb development in the absence of sonic hedgehog function. Dev Biol 236, 421–435. 10.1006/dbio.2001.0346. [PubMed: 11476582]

Chiang C, Litingtung Y, Lee E, Young KE, Corden JL, Westphal H, and Beachy PA. (1996). Cyclopia and defective axial patterning in mice lacking Sonic hedgehog gene function. Nature 383, 407–413. 10.1038/383407a0. [PubMed: 8837770]

Choi HMT, Schwarzkopf M, Fornace ME, Acharya A, Artavanis G, Stegmaier J, Cunha A, and Pierce NA. (2018). Third-generation in situ hybridization chain reaction: multiplexed, quantitative, sensitive, versatile, robust. Development 145. 10.1242/dev.165753.

Dahn RD, and Fallon JF. (2000). Interdigital regulation of digit identity and homeotic transformation by modulated BMP signaling. Science 289, 438–441. 10.1126/science.289.5478.438. [PubMed: 10903202]

Davis AP, Witte DP, Hsieh-Li HM, Potter SS, and Capecchi MR. (1995). Absence of radius and ulna in mice lacking hoxa-11 and hoxd-11. Nature 375, 791–795. 10.1038/375791a0. [PubMed: 7596412]

Drossopoulou G, Lewis KE, Sanz-Ezquerro JJ, Nikbakht N, McMahon AP, Hofmann C, and Tickle C. (2000). A model for anteroposterior patterning of the vertebrate limb based on sequential long- and short-range Shh signalling and Bmp signalling. Development 127, 1337–1348. [PubMed: 10704381]

Author Manuscript Author Manuscript Author Manuscript Author Manuscript

Fromental-Ramain C, Warot X, Messadecq N, LeMeur M, Dolle P, and Chambon P. (1996). Hoxa-13 and Hoxd-13 play a crucial role in the patterning of the limb autopod. Development 122, 2997–3011. [PubMed: 8898214]

Galli A, Robay D, Osterwalder M, Bao X, Benazet JD, Tariq M, Paro R, Mackem S, and Zeller R. (2010). Distinct roles of Hand2 in initiating polarity and posterior Shh expression during the onset of mouse limb bud development. PLoS Genet 6, e1000901. 10.1371/journal.pgen.1000901.

Gao B, Hu J, Stricker S, Cheung M, Ma G, Law KF, Witte F, Briscoe J, Mundlos S, He L, et al. (2009). A mutation in Ihh that causes digit abnormalities alters its signalling capacity and range. Nature 458, 1196–1200. 10.1038/nature07862. [PubMed: 19252479]

Haraguchi R, Motoyama J, Sasaki H, Satoh Y, Miyagawa S, Nakagata N, Moon A, and Yamada G. (2007). Molecular analysis of coordinated bladder and urogenital organ formation by Hedgehog signaling. Development 134, 525–533. 10.1242/dev.02736. [PubMed: 17202190]

Harfe BD, Scherz PJ, Nissim S, Tian F, McMahon AP, and Tabin CJ. (2004). Evidence for an expansion-based temporal Shh gradient in specifying vertebrate digit identities. Cell 118, 517528. Doi 10.1016/J.Cell.2004.07.024.

Harris MP. (2021). Bioelectric signaling as a unique regulator of development and regeneration. Development 148. 10.1242/dev.180794.

Hasson P, Del Buono J, and Logan MP. (2007). Tbx5 is dispensable for forelimb outgrowth. Development 134, 85–92. 10.1242/dev.02622. [PubMed: 17138667]

Huang BL, and Mackem S. (2021). Rethinking positional information and digit identity: The role of late interdigit signaling. Dev Dyn. 10.1002/dvdy.440.

Huang BL, Trofka A, Furusawa A, Norrie JL, Rabinowitz AH, Vokes SA, Mark Taketo M, Zakany J, and Mackem S. (2016). An interdigit signalling centre instructs coordinate phalanx-joint formation governed by 5'Hoxd-Gli3 antagonism. Nat Commun 7, 12903. 10.1038/ncomms12903. [PubMed: 27713395]

Jeong J, Mao J, Tenzen T, Kottmann AH, and McMahon AP. (2004). Hedgehog signaling in the neural crest cells regulates the patterning and growth of facial primordia. Genes Dev 18, 937–951. 10.1101/gad.1190304. [PubMed: 15107405]

Kessel M, and Gruss P. (1991). Homeotic transformations of murine vertebrae and concomitant alteration of Hox codes induced by retinoic acid. Cell 67, 89–104. 10.1016/0092-8674(91)90574i. [PubMed: 1680565]

Kong JH, Siebold C, and Rohatgi R. (2019). Biochemical mechanisms of vertebrate hedgehog signaling. Development 146. 10.1242/dev.166892.

Lewandowski JP, Du F, Zhang S, Powell MB, Falkenstein KN, Ji H, and Vokes SA. (2015). Spatiotemporal regulation of GLI target genes in the mammalian limb bud. Dev Biol 406, 92–103. 10.1016/j.ydbio.2015.07.022. [PubMed: 26238476]

Lewis PM, Dunn MP, McMahon JA, Logan M, Martin JF, St-Jacques B, and McMahon AP. (2001). Cholesterol modification of sonic hedgehog is required for long-range signaling activity and effective modulation of signaling by Ptc1. Cell 105, 599–612. 10.1016/s0092-8674(01)00369-5. [PubMed: 11389830]

Lex RK, Ji Z, Falkenstein KN, Zhou W, Henry JL, Ji H, and Vokes SA. (2020). GLI transcriptional repression regulates tissue-specific enhancer activity in response to Hedgehog signaling. Elife 9, e50670. 10.7554/eLife.50670.

Lex RK, Zhou W, Ji Z, Falkenstein KN, Schuler KE, Windsor KE, Kim JD, Ji H, and Vokes SA. (2022). GLI transcriptional repression is inert prior to Hedgehog pathway activation. Nat Commun 13, 808. 10.1038/s41467-022-28485-4. [PubMed: 35145123]

Li DY, Sakuma R, Vakili NA, Mo R, Puviindran V, Deimling S, Zhang XY, Hopyan S, and Hui CC. (2014). Formation of Proximal and Anterior Limb Skeleton Requires Early Function of Irx3 and Irx5 and Is Negatively Regulated by Shh Signaling. Developmental Cell 29, 233–240. 10.1016/j.devcel.2014.03.001. [PubMed: 24726282]

Lindsten T, Ross AJ, King A, Zong WX, Rathmell JC, Shiels HA, Ulrich E, Waymire KG, Mahar P, Frauwirth K, et al. (2000). The combined functions of proapoptotic Bcl-2 family members bak and bax are essential for normal development of multiple tissues. Mol Cell 6, 1389–1399. 10.1016/s1097-2765(00)00136-2. [PubMed: 11163212]

Author Manuscript Author Manuscript Author Manuscript Author Manuscript

Litingtung Y, Dahn RD, Li Y, Fallon JF, and Chiang C. (2002). Shh and Gli3 are dispensable for limb skeleton formation but regulate digit number and identity. Nature 418, 979–983. 10.1038/nature01033. [PubMed: 12198547]

Logan M, Martin JF, Nagy A, Lobe C, Olson EN, and Tabin CJ. (2002). Expression of Cre Recombinase in the developing mouse limb bud driven by a Prx1 enhancer. Genesis 33, 77–80. 10.1002/gene.10092. [PubMed: 12112875]

Long F, Zhang XM, Karp S, Yang Y, and McMahon AP. (2001). Genetic manipulation of hedgehog signaling in the endochondral skeleton reveals a direct role in the regulation of chondrocyte proliferation. Development 128, 5099–5108. [PubMed: 11748145]

Mariani FV, Ahn CP, and Martin GR. (2008). Genetic evidence that FGFs have an instructive role in limb proximal-distal patterning. Nature 453, 401–405. 10.1038/nature06876. [PubMed: 18449196]

Nacu E, Gromberg E, Oliveira CR, Drechsel D, and Tanaka EM. (2016). FGF8 and SHH substitute for anterior-posterior tissue interactions to induce limb regeneration. Nature 533, 407–410. 10.1038/nature17972. [PubMed: 27120163]

Nakamura E, Nguyen MT, and Mackem S. (2006). Kinetics of tamoxifen-regulated Cre activity in mice using a cartilage-specific CreER(T) to assay temporal activity windows along the proximodistal limb skeleton. Dev Dyn 235, 2603–2612. 10.1002/dvdy.20892. [PubMed: 16894608]

Nguyen MT, Zhu J, Nakamura E, Bao X, and Mackem S. (2009). Tamoxifen-dependent, inducible Hoxb6CreERT recombinase function in lateral plate and limb mesoderm, CNS isthmic organizer, posterior trunk neural crest, hindgut, and tailbud. Dev Dyn 238, 467–474. 10.1002/dvdy.21846. [PubMed: 19161221]

Osterwalder M, Speziale D, Shoukry M, Mohan R, Ivanek R, Kohler M, Beisel C, Wen X, Scales SJ, Christoffels VM, et al. (2014). HAND2 targets define a network of transcriptional regulators that compartmentalize the early limb bud mesenchyme. Dev Cell 31, 345–357. 10.1016/j.devcel.2014.09.018. [PubMed: 25453830]

Panman L, Galli A, Lagarde N, Michos O, Soete G, Zuniga A, and Zeller R. (2006). Differential regulation of gene expression in the digit forming area of the mouse limb bud by SHH and gremlin 1/FGF-mediated epithelial-mesenchymal signalling. Development 133, 3419–3428. 10.1242/dev.02529. [PubMed: 16908629]

Perriton CL, Powles N, Chiang C, Maconochie MK, and Cohn MJ. (2002). Sonic hedgehog signaling from the urethral epithelium controls external genital development. Dev Biol 247, 26–46. 10.1006/dbio.2002.0668 [PubMed: 12074550]

Piccolo S, Sladitschek-Martens HL, and Cordenonsi M. (2022). Mechanosignaling in vertebrate development. Dev Biol 488, 54–67. 10.1016/j.ydbio.2022.05.005. [PubMed: 35580730]

Pickering J, Chinnaiya K, and Towers M. (2019). An autoregulatory cell cycle timer integrates growth and specification in chick wing digit development. Elife 8, e47625. 10.7554/eLife.47625.

Probst S, Kraemer C, Demougin P, Sheth R, Martin GR, Shiratori H, Hamada H, Iber D, Zeller R, and Zuniga A. (2011). SHH propagates distal limb bud development by enhancing CYP26B1-mediated retinoic acid clearance via AER-FGF signalling. Development 138, 1913–1923. 10.1242/dev.063966. [PubMed: 21471156]

Scherz PJ, McGlinn E, Nissim S, and Tabin CJ. (2007). Extended exposure to Sonic hedgehog is required for patterning the posterior digits of the vertebrate limb. Dev Biol 308, 343–354. 10.1016/j.ydbio.2007.05.030. [PubMed: 17610861]

Shapiro MD, Hanken J, and Rosenthal N. (2003). Developmental basis of evolutionary digit loss in the Australian lizard Hemiergis. J Exp Zool B Mol Dev Evol 297, 48–56. 10.1002/jez.b.19. [PubMed: 12955843]

Soriano P. (1999). Generalized lacZ expression with the ROSA26 Cre reporter strain. Nat Genet 21, 70–71. Doi 10.1038/5007. [PubMed: 9916792]

Srinivas S, Watanabe T, Lin CS, William CM, Tanabe Y, Jessell TM, and Costantini F. (2001). Cre reporter strains produced by targeted insertion of EYFP and ECFP into the ROSA26 locus. BMC developmental biology 1, 4. [PubMed: 11299042]

Author Manuscript Author Manuscript Author Manuscript Author Manuscript

Suzuki T, Hasso SM, and Fallon JF. (2008). Unique SMAD1/5/8 activity at the phalanx-forming region determines digit identity. Proc Natl Acad Sci U S A 105, 4185–4190. 10.1073/pnas.0707899105. [PubMed: 18334652]

Takeuchi O, Fisher J, Suh H, Harada H, Malynn BA, and Korsmeyer SJ. (2005). Essential role of BAX,BAK in B cell homeostasis and prevention of autoimmune disease. Proc Natl Acad Sci U S A 102, 11272–11277. 10.1073/pnas.0504783102. [PubMed: 16055554]

Tam PP. (1981). The control of somitogenesis in mouse embryos. J Embryol Exp Morphol 65 *Suppl*, 103–128. [PubMed: 6801176]

Tarchini B, and Duboule D. (2006). Control of Hoxd genes' collinearity during early limb development. Dev Cell 10, 93–103. 10.1016/j.devcel.2005.11.014. [PubMed: 16399081]

te Welscher P, Fernandez-Teran M, Ros MA, and Zeller R. (2002a). Mutual genetic antagonism involving GLI3 and dHAND prepatterns the vertebrate limb bud mesenchyme prior to SHH signaling. Genes Dev 16, 421–426. 10.1101/gad.219202. [PubMed: 11850405]

te Welscher P, Zuniga A, Kuijper S, Drenth T, Goedemans HJ, Meijlink F, and Zeller R. (2002b). Progression of vertebrate limb development through SHH-mediated counteraction of GLI3. Science 298, 827–830. 10.1126/science.1075620. [PubMed: 12215652]

Towers M, Mahood R, Yin Y, and Tickle C. (2008). Integration of growth and specification in chick wing digit-patterning. Nature 452, 882–886. 10.1038/nature06718. [PubMed: 18354396]

Towers M, Signolet J, Sherman A, Sang H, and Tickle C. (2011). Insights into bird wing evolution and digit specification from polarizing region fate maps. Nat Commun 2, 426. 10.1038/ncomms1437. [PubMed: 21829188]

Vokes SA, Ji H, Wong WH, and McMahon AP. (2008). A genome-scale analysis of the cisregulatory circuitry underlying sonic hedgehog-mediated patterning of the mammalian limb. Genes Dev 22, 2651–2663. 10.1101/gad.1693008. [PubMed: 18832070]

Wang B, Fallon JF, and Beachy PA. (2000). Hedgehog-regulated processing of Gli3 produces an anterior/posterior repressor gradient in the developing vertebrate limb. Cell 100, 423–434. 10.1016/s0092-8674(00)80678-9. [PubMed: 10693759]

Wang C, Pan Y, and Wang B. (2010). Suppressor of fused and Spop regulate the stability, processing and function of Gli2 and Gli3 full-length activators but not their repressors. Development 137, 2001–2009. 10.1242/dev.052126. [PubMed: 20463034]

Wilkinson D. (1992). Whole mount in situ hybridization of vertebrate embryos. In In Situ Hybridization: A practical Approach, Wilkinson DG, ed. (Oxford: IRL Press), pp. 75–83.

Witte F, Chan D, Economides AN, Mundlos S, and Stricker S. (2010). Receptor tyrosine kinase-like orphan receptor 2 (ROR2) and Indian hedgehog regulate digit outgrowth mediated by the phalanx-forming region. Proc Natl Acad Sci U S A 107, 14211–14216. 10.1073/pnas.1009314107. [PubMed: 20660756]

Wu X, Zhang LS, Toombs J, Kuo YC, Piazza JT, Tuladhar R, Barrett Q, Fan CW, Zhang X, Walensky LD, et al. (2017). Extra-mitochondrial prosurvival BCL-2 proteins regulate gene transcription by inhibiting the SUFU tumour suppressor. Nat Cell Biol 19, 1226–1236. 10.1038/ncb3616. [PubMed: 28945232]

Yang Y, Drossopoulou G, Chuang PT, Duprez D, Marti E, Bumcrot D, Vargesson N, Clarke J, Niswander L, McMahon A, and Tickle C. (1997). Relationship between dose, distance and time in Sonic Hedgehog-mediated regulation of anteroposterior polarity in the chick limb. Development 124, 4393–4404. [PubMed: 9334287]

Zhang XM, Ramalho-Santos M, and McMahon AP. (2001). Smoothened mutants reveal redundant roles for Shh and Ihh signaling including regulation of L/R symmetry by the mouse node. Cell 106, 781–792. [PubMed: 11517919]

Zhu J, and Mackem S. (2017). John Saunders' ZPA, Sonic hedgehog and digit identity - How does it really all work? Dev Biol 429, 391–400. 10.1016/j.ydbio.2017.02.001. [PubMed: 28161524]

Zhu J, Nakamura E, Nguyen MT, Bao X, Akiyama H, and Mackem S. (2008). Uncoupling Sonic hedgehog control of pattern and expansion of the developing limb bud. Dev Cell 14, 624–632. 10.1016/j.devcel.2008.01.008. [PubMed: 18410737]

Author Manuscript Author Manuscript Author Manuscript Author Manuscript

Zuniga A, Haramis AP, McMahon AP, and Zeller R. (1999). Signal relay by BMP antagonism controls the SHH/FGF4 feedback loop in vertebrate limb buds. Nature 401, 598–602. 10.1038/44157. [PubMed: 10524628]

Author Manuscript
Author Manuscript
Author Manuscript
Author Manuscript

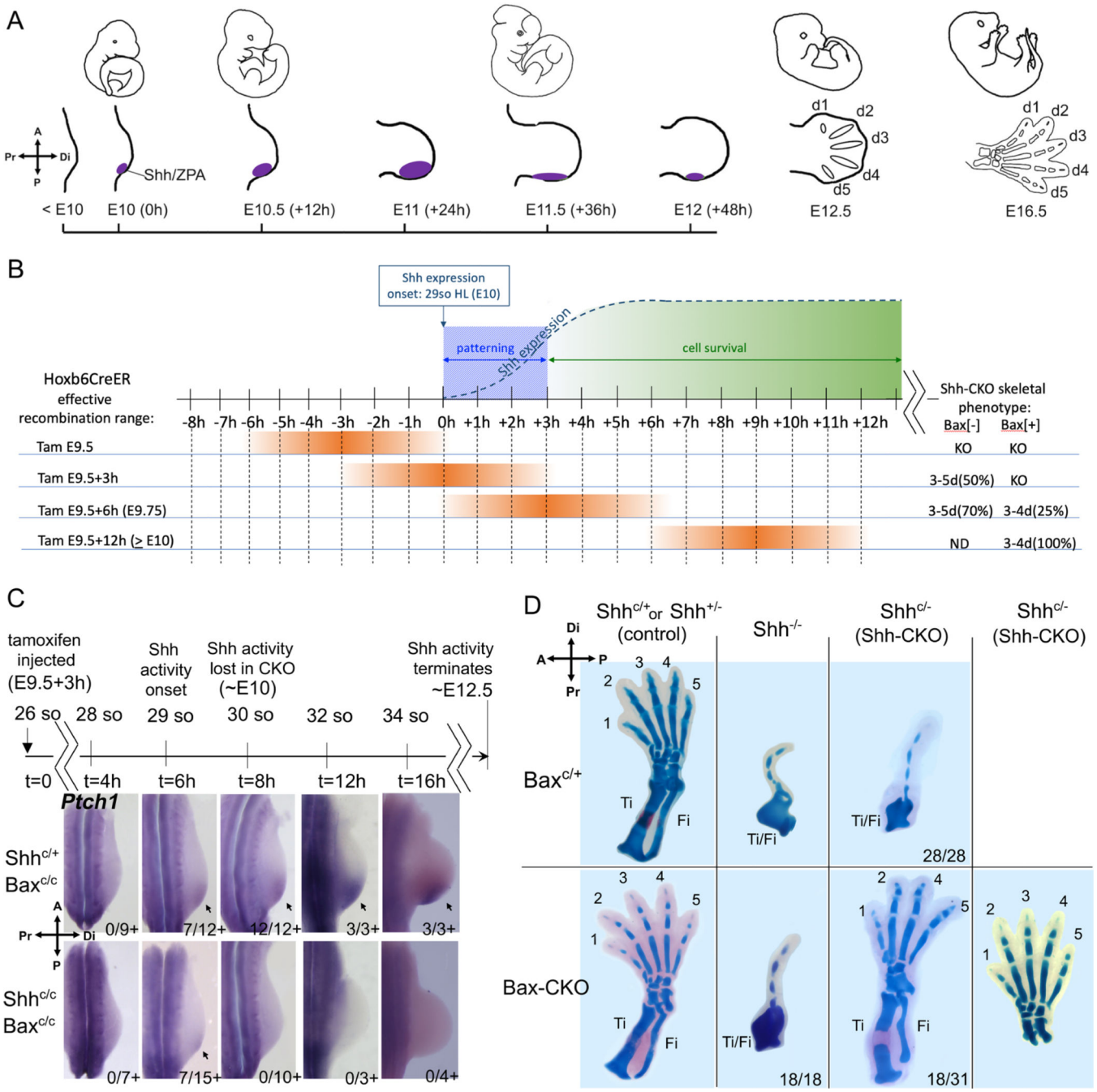

Figure 1. A transient Shh activity pulse suffices to specify all digits with enforced cell survival.

(A) Shh expression timeline in wildtype mouse hindlimb (Shh/ZPA, purple). Limb axis orientation indicated by compasses (upper left) in all figures. **(B)** Summary of recombination timelines (orange; see Methods for somite (so) staging/range) for tamoxifen (Tam)-induced *Shh* deletion at different times relative to Shh expression onset and subsequent digit outcomes (at right); KO, *Shh* null phenotype; ND, not done. At E9.5 Tam, deletion precedes S*hh* expression and all limbs have a *Shh* null phenotype. By E9.75 and later, deletion occurs after the Shh role in maintaining cell survival has commenced and both Bax[+]

Author Manuscript Author Manuscript Author Manuscript Author Manuscript

(apoptosis competent) and Bax[-] (cell survival enforced) embryos display some rescue of digit formation (see Table S1); >E10 data summarized from Zhu et al (2008). **(C)** Shh activity assayed by *Ptch1* RNA (arrows) at times after Tam as indicated on timeline. Shh activity was first detected at 6hr (29 so) after injection in a subset of both control $Shh^{+/C}$;*Bax*-CKO (7/12+), and *Shh*-CKO;*Bax*-CKO (7/15+) embryos, and became robust by 8hr (30 so) in control (12/12+), but was absent in all *Shh*-CKO;*Bax*-CKO embryos (0/10+) from t=8hrs (30 so) and later. **(D)** Skeletal staining (E16.5) after *Bax/Bak* and *Shh* removal by Tam (treated at E9.5+3h, as in **C**). In hindlimbs with *Bax/Bak* present ($Bax^{c/+}$) all *Shh*-CKO embryos (28/28) have *Shh* null phenotype. In hindlimbs with *Bax/Bak* absent (Bax-CKO), about 50% of the *Shh*-CKO embryos (18/31) have 3–5 normal digits (5-digit phenotype shown in right-most panel) and normal zeugopod bones (tibia, Ti; fibula, Fi), but 100% *Shh* null embryos ($Shh^{-/-}$; 18/18) with *Bax/Bak* removed still retain the null mutant phenotype. Related to Figure S1 and Table S1.

Author Manuscript Author Manuscript Author Manuscript Author Manuscript

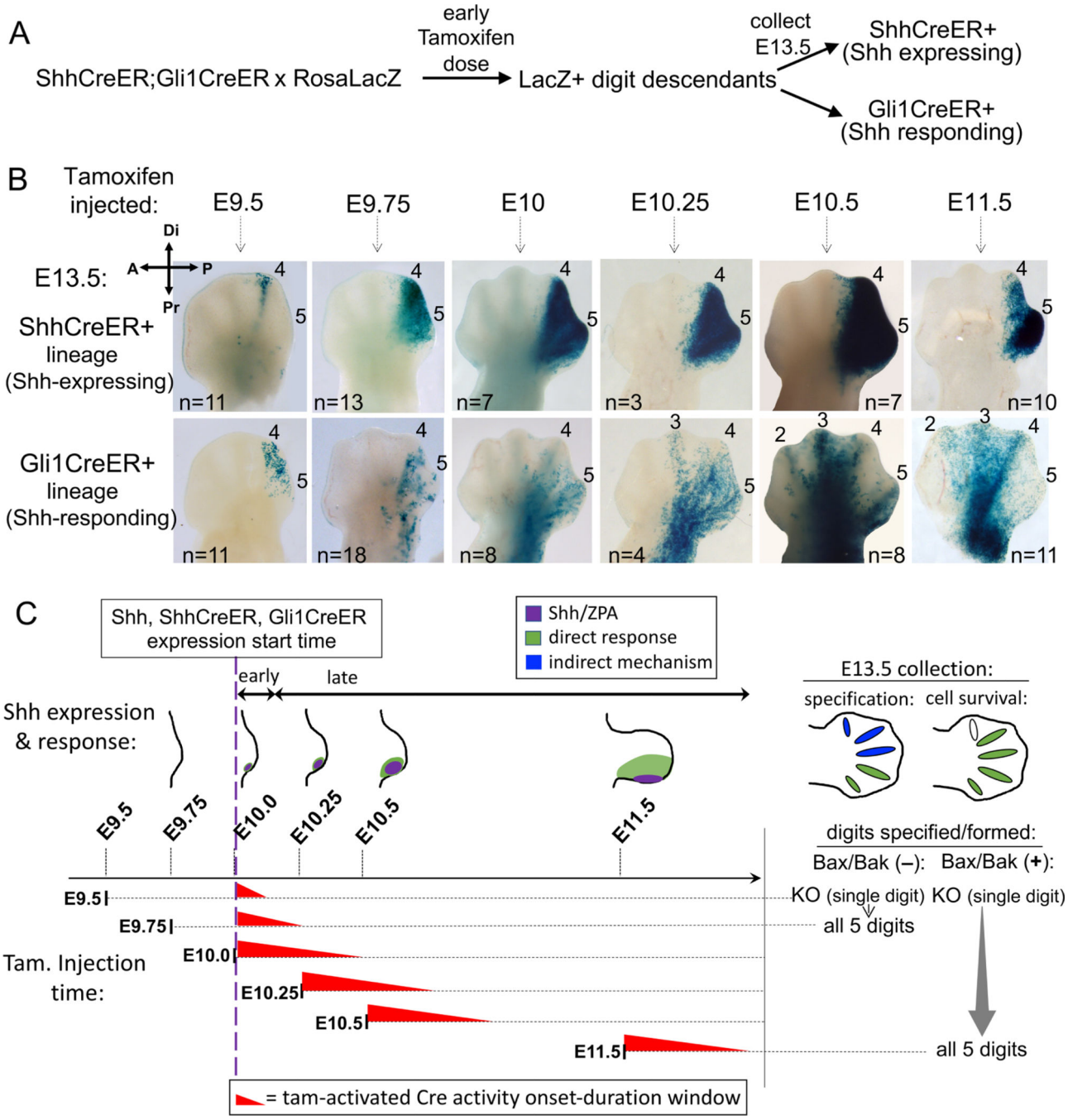

Figure 2. Lineage tracing of *Shh* response in normal limb buds at time of *Shh* onset.

(A) Diagram of strategy to compare Shh-expressing (ShhCreER) and Shh-responding (Gli1CreER) lineages in sibling embryos so that developmental ages and tamoxifen timing are identical. **(B)** Distribution of RosaLacZ reporter+ descendants (in E13.5 digit rays) after single-dose tamoxifen given at time indicated. After E9.5 or E9.75 tamoxifen (time as in Figure 1B), direct Shh-response is limited to digit 4/5 territory (ZPA domain; Shh-expressing descendants). Long-range response in digit 2–3 territory is evident by E10.5. n, numbers analyzed for each dosage time. **(C)** Summary of data in (**B**) showing overlap

Author Manuscript Author Manuscript Author Manuscript Author Manuscript

of tamoxifen (Tam) activity time window (red wedges); Tam duration estimated at ~12hrs (from (Nakamura *et al.*, 2006) and Figures 1B,C, S1A data). *Shh* expression(purple)/direct response(green) in schematics, and summary of digits specified and formed (to right), either with or without enforced cell survival, for same Shh activity time window (from Figure 1, Table S1) for each Tam dosage time. Early-responding cells (Tam at E9.5 or E9.75) contribute only to d4/5 (green, E13.5 hindlimb), indicating d1-d3 are specified by an indirect mechanism (blue). Later stage-responding cells (Tam after E10.25), when Shh acts to maintain cell survival, contribute to d2-d5 (green, E13.5 hindlimb).

Author Manuscript Author Manuscript Author Manuscript Author Manuscript

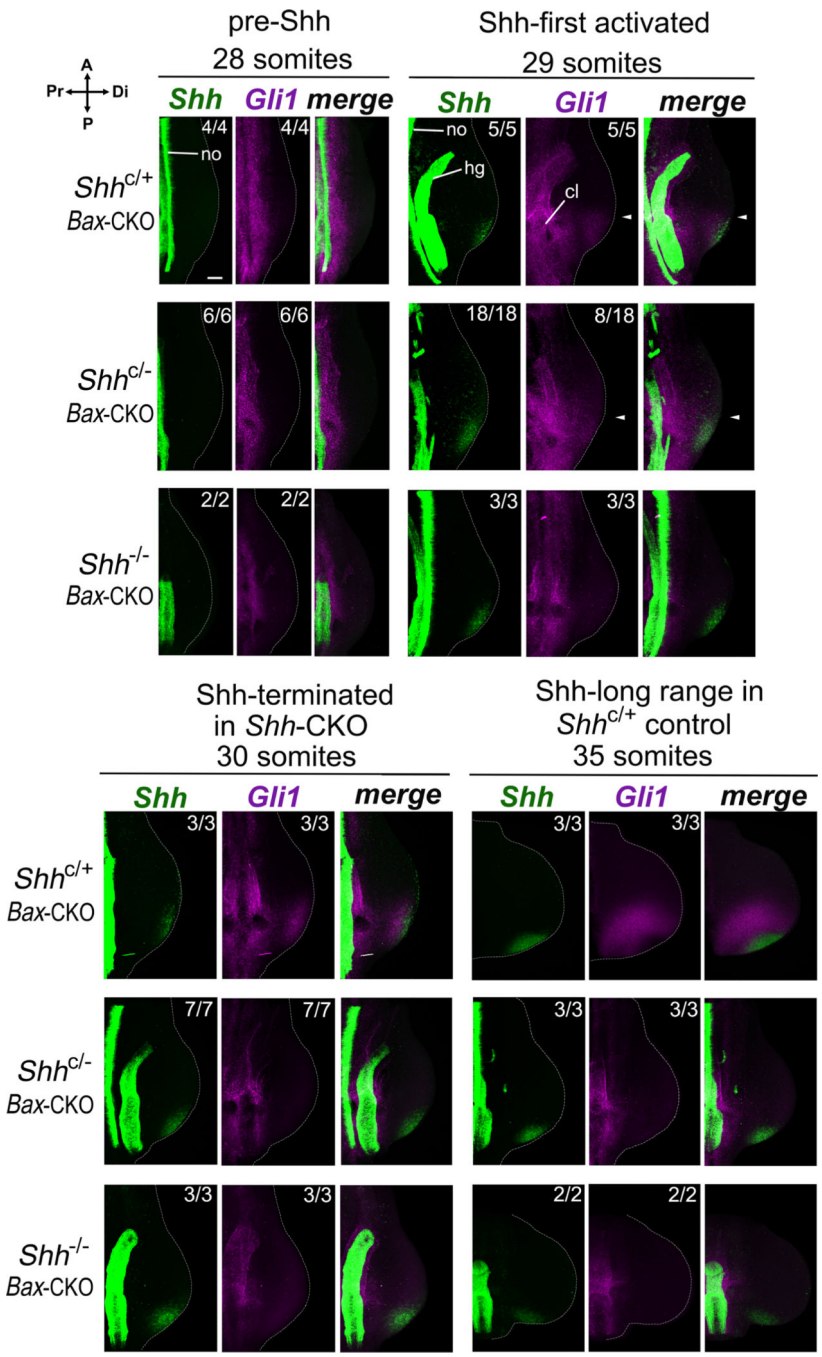

Figure 3. Only short-range Shh response is detected in *Shh*-CKO;*Bax*-CKO embryos during the transient *Shh* expression window.

Shh expression and activity was assayed by *Shh* (green) and *Gli1* (purple) RNA in situ HCR(Choi *et al.*, 2018) at somite stages indicated. After tamoxifen injection at E9.5+3h (as in Figure 1B,C), Shh response (*Gli1*) was detected at the 29 somite stage, shortly after *Shh* expression onset, in all control $Shh^{+/-}$;*Bax*-CKO (5/5) and in a subset of *Shh*-CKO;*Bax*-CKO (8/18) embryos. By 30 somites (2h later) and at 35 somites (12h later), Shh response became robust in all controls but was absent in all *Shh*-CKO embryos. A-P expression extent of *Gli1* in distal limb bud is very similar to that of *Shh* in both the control and the *Shh*-CKO

Author Manuscript Author Manuscript Author Manuscript Author Manuscript

embryos during the transient expression window (29 somites; merged panels, arrows). Note that non-functional (exon 2-deleted) *Shh* RNA remains detectable in both late-stage *Shh*-CKO and in $Shh^{-/-}$ null embryos (with absent *Gli1* RNA signal). Numbers analyzed with result shown are indicated at bottom of each panel, with remainder negative for expression. no, notochord and hg, hindgut axial sources of Hh ligands and cl, cloacal-urogenital region, also responsive to local Shh and Ihh signaling(Haraguchi *et al.*, 2007; Perriton *et al.*, 2002). Scale bar = 100 μm (top left panel; all panels at same scale). Related to Figures 2 and S2.

Author Manuscript Author Manuscript Author Manuscript Author Manuscript

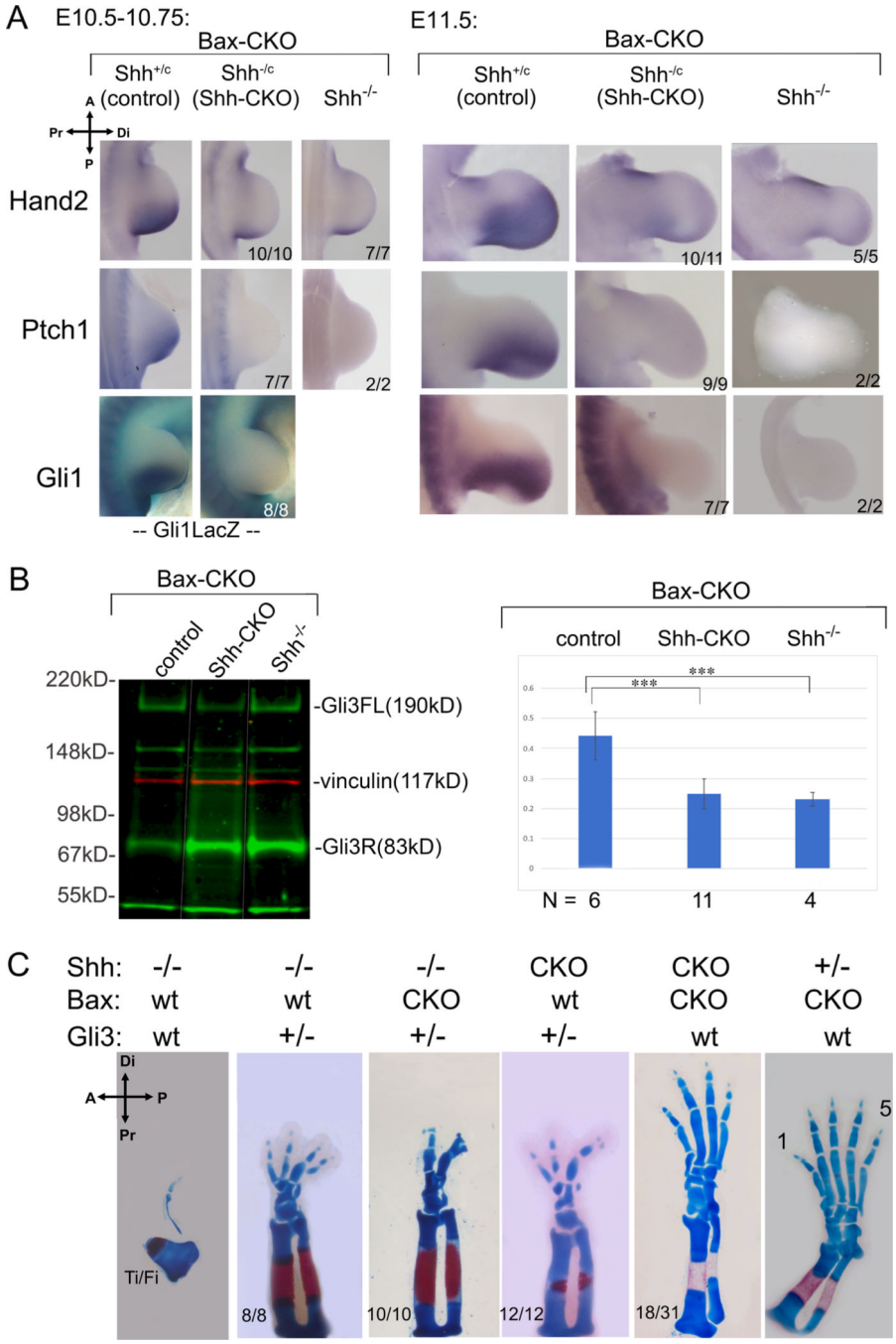

Figure 4. Digit rescue in *Shh*-CKO;*Bax*-CKO embryos is not due to persistent Shh pathway activity or re-activation.

(A) Shh pathway activity monitored by RNA (*Hand2, Ptch1, Gli1*) and by LacZ activity from a *Gli1*$^{LacZ/+}$ knock-in allele after *Shh* removal by tamoxifen at E9.5+3h (as in Figure 1B). Mutant numbers analyzed with result shown are indicated in each panel. *Hand2* at E11.5 was very slightly higher than *Shh*$^{-/-}$ in 1/11 *Shh*-CKO embryos. **(B)** Gli3 full-length (Gli3FL) and repressor (Gli3R) protein quantitation in E10.5 hindlimbs, after *Bax/Bak* and *Shh* removal as in Figure 1B,C. Blot shows representative example of Gli3 level (green)

Author Manuscript Author Manuscript Author Manuscript Author Manuscript

for different genotypes (noncontiguous lanes re-ordered from same blot, indicated by white lines). Molecular weight marker positions indicated to right; vinculin (red) loading control. Gli3 FL/R ratios (mean ± SEM) shown at right in bar-graph with numbers analyzed (N) for each genotype. Gli3 FL/R is equivalently reduced in *Shh*-CKO;*Bax*-CKO (p=0.00002) and in $Shh^{-/-}$;*Bax*-CKO (p=0.001) compared to control, and there is no significant difference in Gli3 FL/R between *Shh*-CKO;*Bax*CKO and $Shh^{-/-}$;*Bax*-CKO (p=0.48). ***, p <0.001. **(C)** Effect of *Gli3* dosage reduction ($Gli3^{+/-}$) on *Shh*-CKO and on $Shh^{-/-}$ skeletal phenotypes (E16.5), compared to the effect of *Bax/Bak* removal (*Bax*-CKO).

Author Manuscript Author Manuscript Author Manuscript Author Manuscript

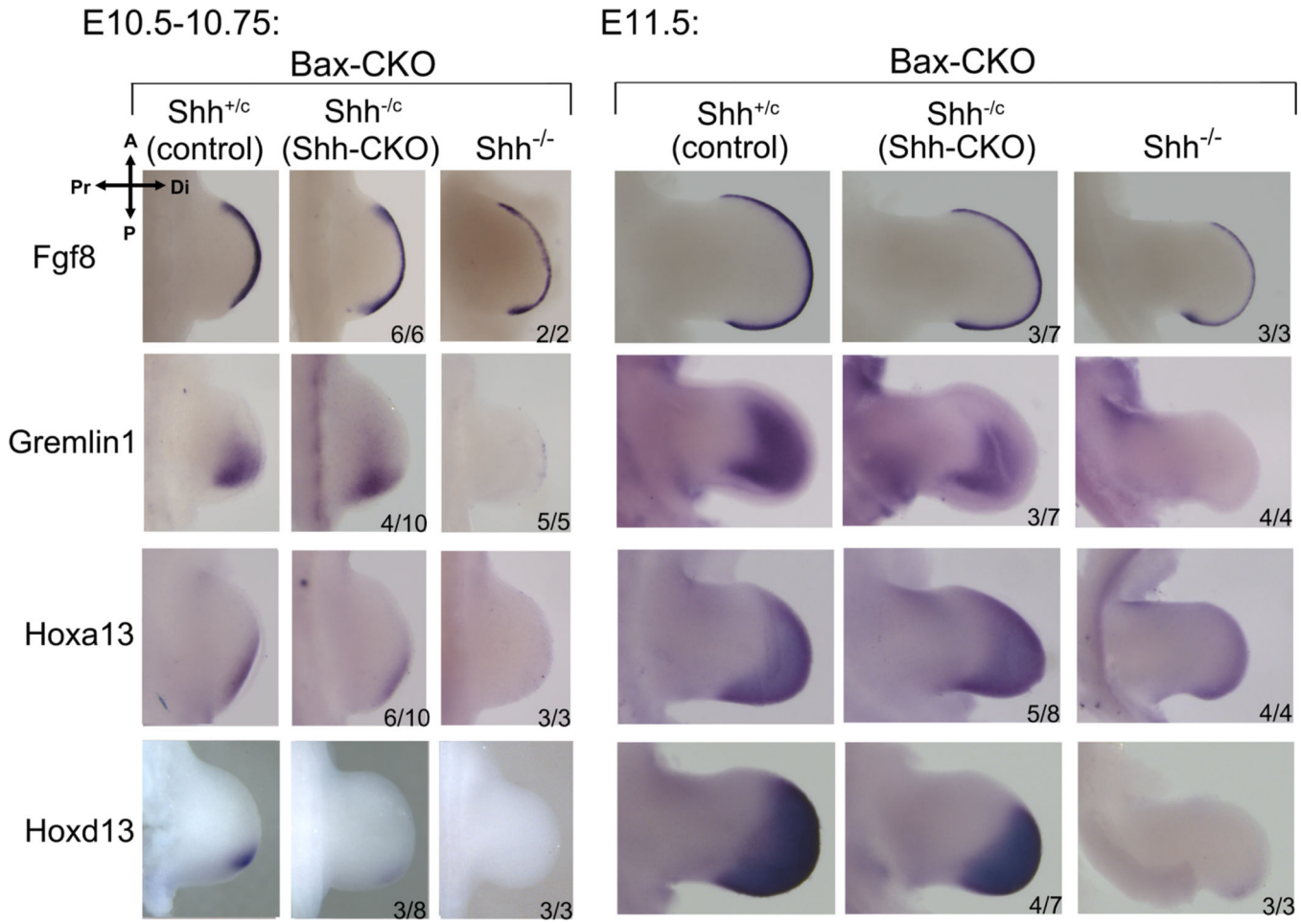

Figure 5. Expression of key targets implicated in outgrowth and patterning is maintained in *Shh*-CKO;*Bax*-CKO embryos.

Expression of Shh target RNAs that regulate outgrowth (*Fgf8, Grem1*) and patterning (*Hoxa13, Hoxd13*) at early and later stages after *Shh* removal by tamoxifen at E9.5+3h (as in Figures 1B, 2A). *Fgf8* expression is unaltered even in $Shh^{-/-}$ null hindlimb at E10.75(Chiang *et al.*, 2001), but was reduced in $Shh^{-/-}$;Bax-CKO by E11.5. *Shh*-CKO;*Bax*-CKO embryo numbers analyzed with result shown are indicated in each panel (expression maintained). In remainder, expression was unchanged from that seen in the null $Shh^{-/-}$;*Bax*-CKO. Related to Figures S3, S4.

Author Manuscript Author Manuscript Author Manuscript Author Manuscript

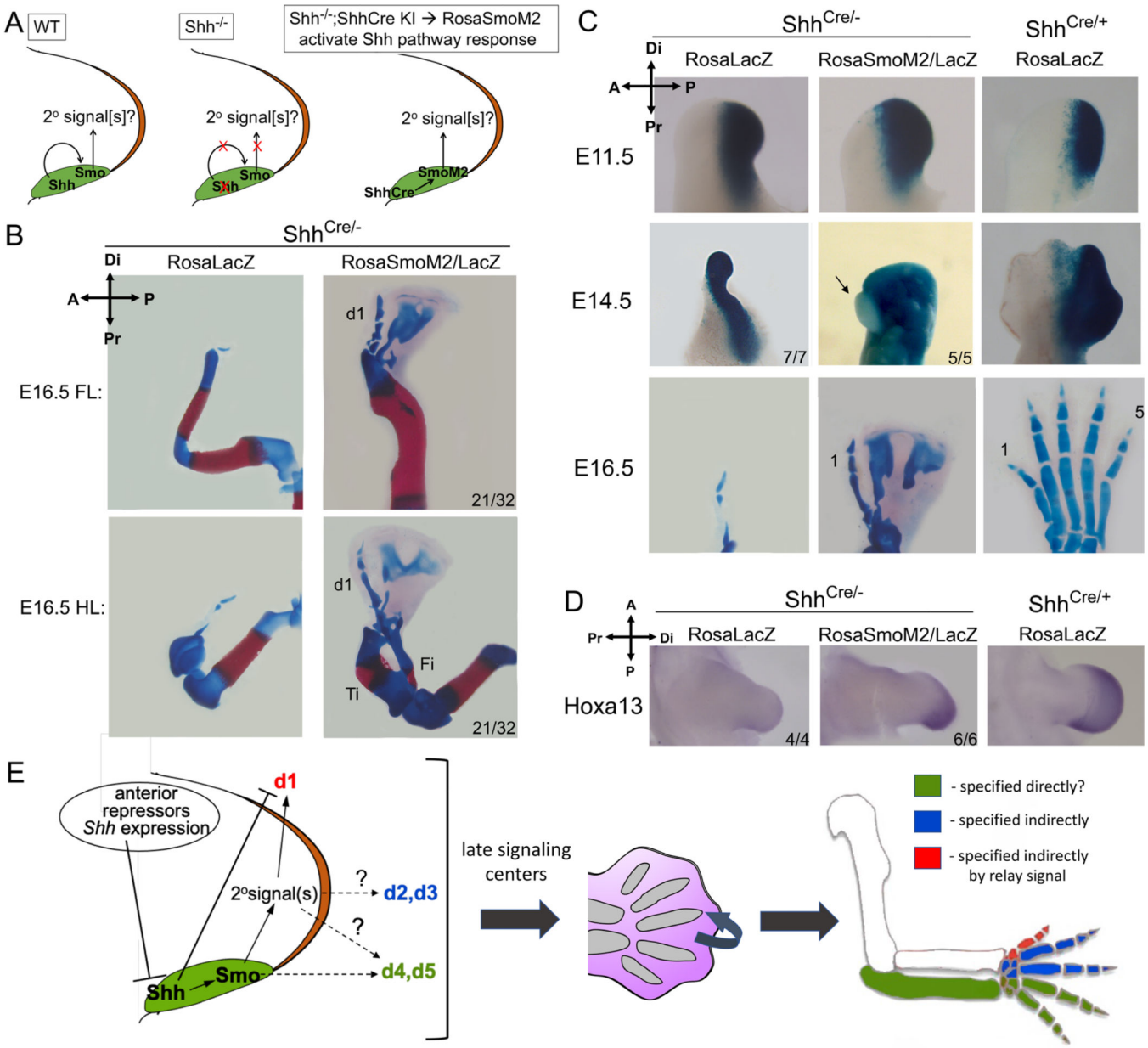

Figure 6. Relay signals downstream of enforced Shh-response confined to ZPA restore normal digit 1 in *Shh*$^{-/-}$ null limb.

(A) diagram of Shh-response activation in ZPA of null limb bud (*Shh*$^{Cre/-}$) by SmoM2 (*Shh*$^{cre/-}$;Shh-SmoM2+). Any effect on non-ZPA digits requires non-autonomous relay signal(s). **(B)** Skeletal stain showing normal digit 1 (d1) in *Shh*$^{cre/-}$;Shh-SmoM2+ forelimbs and hindlimbs (21/32). Ti, tibia; Fi, fibula. **(C)** ZPA-lineage analysis and close-up of mutant footplate with activated SmoM2. The anterior-most digit in *Shh*$^{cre/-}$;Shh-SmoM2+ remains devoid of LacZ+ cells (5/5, arrow), whereas residual digit in *Shh*$^{-/-}$ null arises entirely from LacZ+ ZPA-descended cells (7/7). **(D)** *Hoxa13* RNA is restored in *Shh*$^{cre/-}$;Shh-SmoM2+ (6/6) at E11.5, but is absent in *Shh* null (4/4; forelimb shown). **(E)** Model for digit specification by Shh via indirect mechanisms (see text discussion). Transient Shh specifies

Author Manuscript Author Manuscript Author Manuscript Author Manuscript

non-ZPA digits (d1-d3) by indirect mechanisms. Direct Shh signaling selectively inhibits(Li *et al.*, 2014), but indirect relay signaling promotes, d1 specification, establishing a unique d1 (thumb) regulatory hierarchy. Relay signaling, initiated by early transient Shh, ultimately sets up late interdigit signaling centers to regulate final digit identity. Related to Figure S5.

Author Manuscript Author Manuscript Author Manuscript Author Manuscript

Table 1.

List of genetic crosses, embryo numbers analyzed, and experimental outcomes related to each figure.

Alleles crossed	shorthand notation	%rescue†/analysis	Tam Tx*	phenotype/ analysis	Fig.
Shh$^{+/C}$;*Bax*$^{+/C}$;*Bak*$^{-/-}$;*Hoxb6CreER* x *Shh*$^{C/C}$;*Bax*$^{C/C}$;*Bak*$^{-/-}$;*Hoxb6CreER*	Shh-CKO;Bax-CKO Shh-CKO;Bax$^{+/c}$	18/31 (Bax-KO); 0/28 (Bax-het)	E9.5+3h	skeleton	1
Shh$^{+/-}$;*Bax*$^{+/C}$;*Bak*$^{-/-}$;*Hoxb6CreER* x *Shh*$^{+/-}$;*Bax*$^{C/C}$;*Bak*$^{-/-}$	Shh$^{-/-}$;Bax-CKO	0/18 (Bax-KO)	E8.75–E9.5	skeleton	1
Shh$^{+/-}$;*Bax*$^{+/-}$;*Bak*$^{-/-}$ x *Shh*$^{+/-}$;*Bax*$^{+/-}$;*Bak*$^{-/-}$	Shh$^{-/-}$;Bax$^{-/-}$	0/6 (Bax/Bak-KO)	NA	skeleton	1
Shh$^{+/C}$;*Bax*$^{C/C}$;*Bak*$^{-/-}$;*Hoxb6CreER* x *Shh*$^{C/C}$;*Bax*$^{C/C}$;*Bak*$^{-/-}$;*Hoxb6CreER*	Shh-CKO;Bax-CKO	NA-see Figs. 1, S1, text	E9.5+3h	Shh activity duration	1, S1
Shh$^{+/-}$;*Bax*$^{+/C}$;*Bak*$^{-/-}$;*Hoxb6CreER* x *Shh*$^{-/C}$;*Bax*$^{C/C}$;*Bak*$^{-/-}$;*Hoxb6CreER*	Shh-CKO;Bax-CKO Shh$^{-/-}$;Bax-CKO	NA-see Fig. S1, text	E9.5+3h	Cell survival	S1
Shh$^{CreER/+}$;*Rosa*$^{LacZ/LacZ}$ x *Gli1*$^{CreER/+}$;*Rosa*$^{LacZ/LacZ}$	ShhCreER+ or Gli1CreER+	-51 embryos -60 embryos	Varied-Fig 2	Shh-expression, -response lineage	2
Shh$^{+/-}$;*Bax*$^{C/C}$;*Bak*$^{-/-}$;*Hoxb6CreER* x *Shh*$^{-/C}$;*Bax*$^{C/C}$;*Bak*$^{-/-}$;*Hoxb6CreER*	Shh-CKO;Bax-CKO Shh$^{-/-}$;Bax-CKO	NA-see Figs. 3, S2 text	E9.5+3h	In situ HCR – Shh, Gli1 (response)	3, S2
Shh$^{+/-}$;*Bax*$^{C/C}$;*Bak*$^{-/-}$;*Hoxb6CreER* x *Shh*$^{-/C}$;*Bax*$^{C/C}$;*Bak*$^{-/-}$;*Hoxb6CreER*	Shh-CKO;Bax-CKO Shh$^{-/-}$;Bax-CKO	NA-see Fig. 4, text	E9.5+3h	Hand2, Ptch1, Gli1 Gli3 western	4
Shh$^{+/-}$;*Gli3*$^{+/-}$;*Bax*$^{C/C}$;*Bak*$^{-/-}$;*Hoxb6CreER* x *Shh*$^{+/-}$;*Bax*$^{C/C}$;*Bak*$^{-/-}$;*Hoxb6CreER*	Shh$^{-/-}$;Gli3$^{+/-}$;BaxCKO	10/10 (vs Shh$^{-/-}$)			
Shh$^{+/-}$;*Gli3*$^{+/-}$ x *Shh*$^{+/-}$	Shh$^{-/-}$;Gli3$^{+/-}$	8/8 (vs Shh$^{-/-}$)			
Shh$^{+/-}$;*Gli3*$^{+/-}$ x *Shh*$^{C/C}$;*Hoxb6CreER*	Shh-CKO;Gli3$^{+/-}$	12/12 (vs Shh-CKO)			
Shh$^{+/-}$;*Bax*$^{C/C}$;*Bak*$^{-/-}$;*Hoxb6CreER* x *Shh*$^{-/C}$;*Bax*$^{C/C}$;*Bak*$^{-/-}$;*Hoxb6CreER*	Shh-CKO;Bax-CKO	18/31 (vs Shh-CKO)	NA or E9.5+3h	skeleton - Gli3 dose modulation	4
Shh$^{+/-}$;*Bax*$^{C/C}$;*Bak*$^{-/-}$;*Hoxb6CreER* x *Shh*$^{-/C}$;*Bax*$^{C/C}$;*Bak*$^{-/-}$;*Hoxb6CreER*	Shh-CKO;Bax-CKO Shh$^{-/-}$;Bax-CKO	NA-see Fig. 5, text	E9.5+3h	Fgf8, Grem1, Hoxa13, Hoxd13	5
Shh$^{+/-}$;*Bax*$^{C/C}$;*Bak*$^{-/-}$;*Hoxb6CreER* x *Shh*$^{-/C}$;*Bax*$^{C/C}$;*Bak*$^{-/-}$;*Hoxb6CreER*	Shh-CKO;Bax-CKO Shh$^{-/-}$;Bax-CKO	NA-see Fig. S3, text	E9.5+3h	Jag1, Cyp26b1, Hoxd11, Hoxd13	S3
Shh$^{+/-}$;*Bax*$^{C/C}$;*Bak*$^{-/-}$;*Hoxb6CreER* x *Shh*$^{-/C}$;*Bax*$^{C/C}$;*Bak*$^{-/-}$;*Hoxb6CreER*	Shh-CKO;Bax-CKO Shh$^{-/-}$;Bax-CKO	NA-see Fig. S4, text	E9.5+3h	Anterior pattern genes: Alx4, Irx3	S4
Shh$^{Cre/+}$;*Rosa*$^{LacZ/LacZ}$ x *Shh*$^{+/-}$;*Rosa*$^{SmoM2/SmoM2}$	Shh$^{Cre/-}$;Shh-SmoM2	21/32 (digit 1+)	NA	Skeleton; Hoxa13, Shh-lineage	6
Shh$^{Cre/+}$;*Rosa*$^{LacZ/LacZ}$ x *Shh*$^{+/-}$	Shh$^{Cre/-}$	0/6 (digit 1+)			
Shh$^{Cre/+}$;*Bax*$^{+/-}$;*Bak*$^{-/-}$;*Rosa*$^{LacZ/LacZ}$ x *Shh*$^{+/-}$;*Bax*$^{+/-}$;*Bak*$^{-/-}$;*Rosa*$^{SmoM2/ SmoM2}$	Shh$^{Cre/-}$;Bax/Bak-KO; Shh-SmoM2	8/8 (only digit 1+)	NA	skeleton	6
Shh$^{Cre/+}$;*Rosa*$^{LacZ/LacZ}$ x *Shh*$^{+/-}$;*Rosa*$^{SmoM2/+}$	Shh$^{Cre/+}$;Shh-SmoM2	4/64 (ectopic ZPA, duplicated d1)	NA	skeleton Shh-lineage	S5

Author Manuscript

Author Manuscript

Author Manuscript

Author Manuscript

Alleles crossed	shorthand notation	%rescue[†]/analysis	Tam Tx[*]	phenotype/ analysis	Fig.
	$Shh^{Cre/-}$;Shh-SmoM2 $Shh^{Cre/-}$	NA-see Fig. S5, text		Uncx4.1, Sox9 Ptch1, Gli1	
$Shh^{Cre/+}$;$Rosa^{LacZ/LacZ}$ x $Shh^{+/-}$;$Rosa^{SmoM2/+}$ $Shh^{Cre/+}$;$Rosa^{EYFP/EYFP}$ x $Shh^{+/-}$;$Rosa^{SmoM2/+}$	$Shh^{Cre/-}$;Shh-SmoM2 $Shh^{Cre/-}$	−10 embryos − 6 embryos	NA	Shh-lineage; cell survival	S5

[†] skeletal numbers refer to embryo numbers (left+right hindlimb both rescued);

[*] Tx, treatment time

Author Manuscript Author Manuscript Author Manuscript Author Manuscript

KEY RESOURCES TABLE

REAGENT or RESOURCE	SOURCE	IDENTIFIER
Antibodies		
goat anti-Gli3 antibody	R&D Systems	Cat#AF3690; RRID: AB_2232499
rabbit anti-Gli3 antibody	Chen et al., 2004	N/A
mouse anti-Vinculin antibody	Sigma-Aldrich	Cat#V9264; RRID: AB_10603627
IRDye 800CW goat anti-rabbit secondary antibody	LI-COR	Cat#926-32211; RRID: AB_621843
IRDye 800CW donkey anti-goat secondary antibody	LI-COR	Cat#926-32214; RRID: AB_621846
IRDye 680RD donkey anti-mouse secondary antibody	LI-COR	Cat#926-68072; RRID: AB_10953628
Anti-Digoxigenin-AP antibody	Sigma-Aldrich	Cat#11093274910; RRID: AB_2734716
Chemicals, Peptides, and Recombinant Proteins		
Tamoxifen	Sigma-Aldrich	Cat#T5648; CAS: 10540-29-1
Progesterone	West-Ward Pharmaceuticals	Cat#NDC 0143-9725-01; CAS: 57-83-0
Lysotracker Red	ThermoFisher Scientific	Cat#L7528
Alcian Blue 8 GX	Sigma-Aldrich	Cat#A-5268; CAS: 33864-99-2
Alizarin Red S	Sigma-Aldrich	Cat#A5533; CAS: 130-22-3
Ethanol	Sigma-Aldrich	Cat# 107017; CAS: 64-17-5
Acetone	Sigma-Aldrich	Cat# 179124; CAS: 67-64-1
Methanol	Sigma-Aldrich	Cat#322415; CAS: 67-56-1
Paraformaldehyde	Sigma-Aldrich	Cat#441244; CAS: 30525-89-4
Glutaraldehyde	Polyscience	Cat#00216; CAS: 111-30-8
Glycerol	Sigma-Aldrich	Cat#G7757; CAS: 56-81-5
Formamide	Sigma-Aldrich	Cat#F7503; CAS: 75-12-7
X-Gal	GoldBio	Cat#X4281C; CAS: 7240-90-6
Potassium ferrocyanide	Sigma-Aldrich	Cat#P3289; CAS: 14459-95-1
Potassium ferricyanide	Sigma-Aldrich	Cat#702587; CAS: 13746-66-2
BM-Purple	Sigma-Aldrich	Cat#11442074001
NBT	Sigma-Aldrich	Cat#11383213001; CAS: 298-83-9
BCIP	Sigma-Aldrich	Cat#11383221001; CAS: 6578-06-9
Benzyl alcohol	Sigma-Aldrich	Cat#108006; CAS: 100-51-6
Benzyl benzoate	Sigma-Aldrich	Cat#B6630; CAS: 120-51-4
NuPAGE LDS Sample Buffer (4X)	ThermoFisher Scientific	Cat#NP0007
cOmplete, Mini Protease Inhibitor Cocktail	Sigma-Aldrich	Cat# 11836153001
Critical Commercial Assays		
in situ Hybridization Chain Reaction v3.0	Molecular Instruments (Choi et al., 2018)	N/A
NuPAGE 3 to 8%, Tris-Acetate protein gels	ThermoFisher Scientific	Cat# EA0378BOX

Author Manuscript Author Manuscript Author Manuscript Author Manuscript

REAGENT or RESOURCE	SOURCE	IDENTIFIER
Experimental Models: Organisms/Strains		
Mouse: *Shh*$^{flox/flox}$	The Jackson Laboratory	Cat#004293; RRID:IMSR_JAX:004293
Mouse: *Shh*$^{Cre/+}$	The Jackson Laboratory	Cat#005622; RRID:IMSR_JAX:005622
Mouse: *Shh*$^{CreER/+}$	The Jackson Laboratory	Cat#005623; RRID:IMSR_JAX:005623
Mouse: *Gli1*$^{CreER/+}$	The Jackson Laboratory	Cat#007913; RRID:IMSR_JAX:007913
Mouse: *Bax*$^{flox/flox}$;*Bak*$^{-/-}$	The Jackson Laboratory	Cat#006329; RRID:IMSR_JAX:006329
Mouse: *Prrx-Cre* tg	The Jackson Laboratory	Cat#005584; RRID:IMSR_JAX:005584
Mouse: *Rosa-EYFP* tg	The Jackson Laboratory	Cat#006148; RRID:IMSR_JAX:006148
Mouse: *Rosa-SmoM2*	The Jackson Laboratory	Cat#005130; RRID:IMSR_JAX:005130
Mouse: *Shh*$^{+/-}$	Chiang et al., 1996	N/A
Mouse: *Gli3*$^{XtJ/+}$	Buscher et al., 1998	N/A
Mouse: *Gli1*$^{LacZ/+}$	Bai et al., 2002	N/A
Mouse: *Rosa-LacZ*	Soriano, 1999	N/A
Mouse: *Hoxb6-CreER* tg	Nguyen et al., 2009	N/A
Mouse: *Bax*$^{+/-}$	This study – see STAR method; Table 1	N/A
Oligonucleotides		
Genotyping primers for Bax-deleted allele	This study; 300bp PCR product	F: 5′-GAACCCTAGGACCCCTCCG-3′ R: 5′-CAACTCCTACCGCAAGTCCTGG-3′
Genotyping primers for other mouse lines	Integrated DNA Technologies	Sequence information available from the Jackson Lab website and original published papers
Recombinant DNA		
pBluescript-mGli1	Gift from Dr. A. Joyner; Dev. Biol. Program, Sloan Kettering Institute, NY, NY	N/A
pGEMT-mPtch1	Gift from Dr. H. Arnheiter; NINDS, NIH, Bethesda, MD	N/A
pBluescript-mHand2	Gift from Dr. M. Ros; IBBTEC, Univ. Cantabria, Santander, Spain	N/A
pBluescript-mFgf8	Gift from Dr. G. Martin; UCSF, San Francisco, CA	N/A
pBluescript-mGremlin1	Gift from Dr. Y. Yang; Dept. Dev. Biol., Harvard Sch. Dental Medicine, Boston, MA	N/A
mCyp26b1 ORF clone	Origene Technologies	Cat#MR222344
pGEMT-mHoxd13	Gift from Dr. D. Duboule; Dept. Genetics and Evolution, Univ. Geneva, Switzerland	N/A
pGEMT-mHoxd11	Gift from Dr. D. Duboule;as above	N/A
pXCMI-mHoxa13	Gift from Dr. S. Stadler; Div. Skeletal Biology, Shriners Hospital for Children, Portland,OR	N/A
pBluescript-mJagged1	Gift from Dr. P. Koopman; Inst. Mol. Bioscience, Univ. Queensland, Brisbane, Australia	N/A
pBluescript-mIrx3	Gift from Dr. Kmita; Genetics and Dev. Res. Unit, Institut	N/A

Author Manuscript Author Manuscript Author Manuscript Author Manuscript

REAGENT or RESOURCE	SOURCE	IDENTIFIER
	de Recherches Cliniques de Montréal, Québec, Canada	
pBluescript-mAlx4	Gift from Dr. M. Ros; as above	N/A
pBluescript-mUncx4.1	Gift from Dr. B. Herrmann; Max Planck Inst. for Molecular Genetics, Dept. Dev. Genetics, Berlin, Germany	N/A
pBluescript-mSox9	Gift from Dr. R.R. Behringer; Dept. Mol. Genetics, UT-MDACC, Houston, TX	N/A
Software and Algorithms		
LI-COR Odyssey Image Studio v5.2	LI-COR	RRID: SCR_014579
Imaris v9.1	Bitplane/Oxford Instruments	RRID: SCR_007370
Microsoft excel ver 16.59	Microsoft	N/A